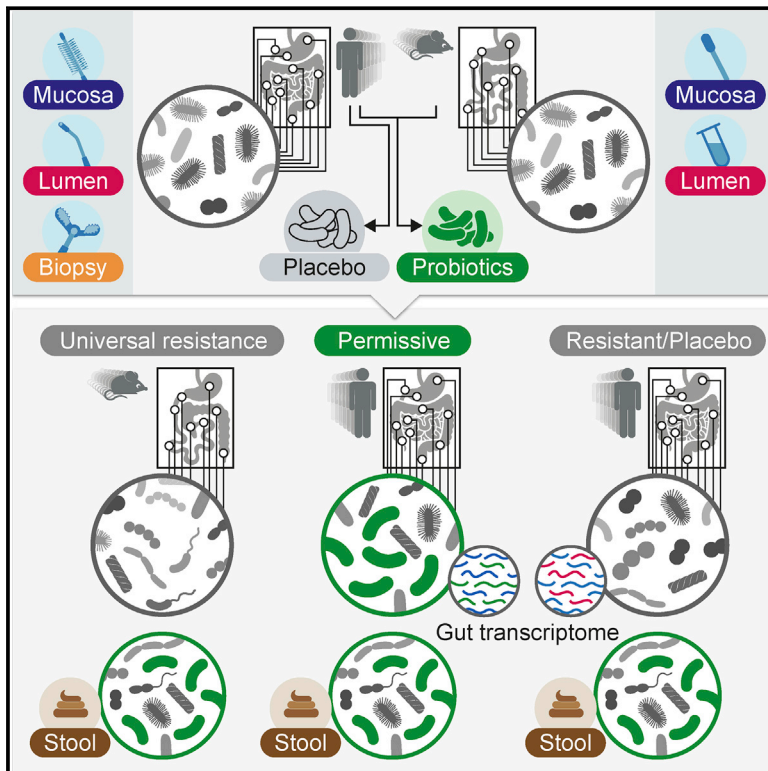# Cell

Personalized Gut Mucosal Colonization Resistance to Empiric Probiotics Is Associated with Unique Host and Microbiome Features

Graphical Abstract

Authors

Niv Zmora, Gili Zilberman-Schapira, Jotham Suez, ..., Zamir Halpern, Eran Segal, Eran Elinav

Correspondence

zamir@tlvmc.gov.il (Z.H.),
eran.segal@weizmann.ac.il (E.S.),
eran.elinav@weizmann.ac.il (E.E.)

In Brief

Probiotics transiently colonize the human gut mucosa in highly individualized patterns, thereby differentially impacting the indigenous microbiome and host gene-expression profile, a trait which is predictable by baseline host and microbiome features, but not by stool shedding.

Highlights

- The murine & human gut mucosal microbiome only partially correlates with stool

- Mice feature an indigenous-microbiome driven colonization resistance to probiotics

- Humans feature a person-specific gut mucosal colonization resistance to probiotics

- Probiotic colonization is predictable by pre-treatment microbiome & host features

CellPress

Personalized Gut Mucosal Colonization Resistance to Empiric Probiotics Is Associated with Unique Host and Microbiome Features

Niv Zmora,[1,2,11] Gili Zilberman-Schapira,[1,11] Jotham Suez,[1,11] Uria Mor,[1,11] Mally Dori-Bachash,[1] Stavros Bashiardes,[1] Eran Kotler,[3,4] Maya Zur,[1] Dana Regev-Lehavi,[1] Rotem Ben-Zeev Brik,[1] Sara Federici,[1] Yotam Cohen,[1] Raquel Linevsky,[1] Daphna Rothschild,[3,4] Andreas E. Moor,[3] Shani Ben-Moshe,[3] Alon Harmelin,[5] Shalev Itzkovitz,[3] Nitsan Maharshak,[6,7,8] Oren Shibolet,[6,7,8] Hagit Shapiro,[1] Meirav Pevsner-Fischer,[1] Itai Sharon,[9,10] Zamir Halpern,[6,7,8,12,*] Eran Segal,[3,4,12,*] and Eran Elinav[1,12,13,*]

[1]Immunology Department, Weizmann Institute of Science, Rehovot, 7610001, Israel
[2]Internal Medicine Department, Tel Aviv Sourasky Medical Center, Tel Aviv, 6423906, Israel
[3]Department of Molecular Cell Biology, Weizmann Institute of Science, Rehovot, 7610001, Israel
[4]Department of Computer Science and Applied Mathematics, Weizmann Institute of Science, Rehovot, 7610001, Israel
[5]Department of Veterinary Resources, Weizmann Institute of Science, Rehovot, 7610001, Israel
[6]Department of Gastroenterology and Liver Diseases, Tel Aviv Sourasky Medical Center, Tel Aviv, 6423906, Israel
[7]Research Center for Digestive Tract and Liver Diseases, Tel Aviv Sourasky Medical Center, Tel Aviv 6423906, Israel
[8]Sackler Faculty of Medicine, Tel Aviv University, Tel Aviv 6997801, Israel
[9]Migal Galilee Research Institute, Kiryat Shmona, 11016, Israel
[10]Tel Hai College, Upper Galilee, 1220800, Israel
[11]These authors contributed equally
[12]Senior author
[13]Lead contact
*Correspondence: zamir@tlvmc.gov.il (Z.H.), eran.segal@weizmann.ac.il (E.S.), eran.elinav@weizmann.ac.il (E.E.)
https://doi.org/10.1016/j.cell.2018.08.041

SUMMARY

Empiric probiotics are commonly consumed by healthy individuals as means of life quality improvement and disease prevention. However, evidence of probiotic gut mucosal colonization efficacy remains sparse and controversial. We metagenomically characterized the murine and human mucosal-associated gastrointestinal microbiome and found it to only partially correlate with stool microbiome. A sequential invasive multi-omics measurement at baseline and during consumption of an 11-strain probiotic combination or placebo demonstrated that probiotics remain viable upon gastrointestinal passage. In colonized, but not germ-free mice, probiotics encountered a marked mucosal colonization resistance. In contrast, humans featured person-, region- and strain-specific mucosal colonization patterns, hallmarked by predictive baseline host and microbiome features, but indistinguishable by probiotics presence in stool. Consequently, probiotics induced a transient, individualized impact on mucosal community structure and gut transcriptome. Collectively, empiric probiotics supplementation may be limited in universally and persistently impacting the gut mucosa, meriting development of new personalized probiotic approaches.

INTRODUCTION

Dietary live bacteria supplementation, collectively termed probiotic therapy, constitutes a continuously growing market. Recent estimates suggest that 3.9 million adults in the US consume prebiotic or probiotic supplements, while up to 60% of healthcare providers prescribe probiotics to their patients (Draper et al., 2017), making probiotics one of the most commonly consumed dietary supplements (Clarke et al., 2015). Rationales for probiotics consumption by healthy individuals include alleviation of gastrointestinal (GI) symptoms (Guyonnet et al., 2009), "fortification" of the immune system (Fukushima et al., 1998), protection against infectious diseases (Panigrahi et al., 2017), prevention of cardio-metabolic disease (Sun and Buys, 2016, Zhang et al., 2015), mental and behavioral augmentation, and promotion of wellbeing (McKean et al., 2017). However, there is great need in additional evidence-based proof of such probiotics impacts in humans (Senok et al., 2005).

Similarly, the efficacy of probiotics in treating infections or existing conditions such as cardio-metabolic or inflammatory bowel diseases remains highly debated (Rondanelli et al., 2017, Crovesy et al., 2017), and some studies have even reported probiotics-associated morbidity and mortality (Besselink et al., 2008, Honeycutt et al., 2007, Vogel, 2008). Importantly, adverse effects associated with probiotic consumption may be under-reported in clinical trials (Bafeta et al., 2018). Medical authorities, such as the European Food Safety Authority (Rijkers et al., 2011) or the US Food and Drug Administration (Saldanha, 2008), have therefore declined to approve probiotic formulations as medical intervention modalities, and they are often classified

as dietary supplements, emphasizing their safety, viability during passage through the GI tract and lack of impact on food taste (Tuomola et al., 2001), rather than providing concrete and reproducible evidence of health-promoting effects (Degnan, 2012).

Do exogenous bacteria colonize the human GI tract and in particular the mucosa-associated surfaces? Some studies suggest that probiotics are globally shed in stool, in a period confined to the time of administration and shortly thereafter (Sierra et al., 2010, Wang et al., 2015, Rochet et al., 2006, Goossens et al., 2003, Lahti et al., 2013, Jacobsen et al., 1999, Tannock et al., 2000). Others suggest generalized (Goldin et al., 1992) or subset-specific (Maldonado-Gómez et al., 2016) probiotic shedding in stool even after consumption ceases. Although *in vitro* studies suggest that probiotics can adhere to human intestinal epithelium (Turroni et al., 2013, Kaushik et al., 2009), these studies are susceptible to bias related to bacterial concentrations, growth stage, incubation time, and growth medium (Van Tassell and Miller, 2011, Lee et al., 2000, Bernet et al., 1994), and are not physiological (He et al., 2001). The spatial and modulatory effects of probiotics on the indigenous microbiome are equally elusive. A recent systematic review reported no effect of probiotics on fecal microbiome composition in six out of seven analyzed studies (Kristensen et al., 2016), coinciding with additional recent works (Maldonado-Gómez et al., 2016, Laursen et al., 2017, Eloe-Fadrosh et al., 2015). Conversely, other works observed alterations in the fecal microbiome composition of probiotics-treated individuals (Ferrario et al., 2014, Goossens et al., 2006, Wang et al., 2015, Martin et al., 2008). Importantly, no study has so far investigated the probiotics effects on the mucosal GI microbiome functionality.

A comprehensive assessment of probiotic effects on the mammalian host is therefore of great necessity to researchers, caregivers, and consumers, but is associated with several significant challenges. First, it would need to go beyond using 16S rDNA analysis alone to distinguish between probiotic and similar endogenous strains, or to quantify impacts on microbiome function, especially as probiotics can have strain-specific or composite properties and effects (Yuan et al., 2017, Hegarty et al., 2017, Maldonado-Gómez et al., 2016, Tannock et al., 2000, Goldin et al., 1992). Second, significant inter-individual human microbiome variability mediated by factors such as age, diet, antibiotic usage, food supplements, underlying medical conditions, and patterns of circadian activity (Zmora et al., 2016) can impact effects of probiotics. Third, stool microbiome assessments are not necessarily a surrogate marker for the effects of GI mucosal probiotics on the host and its microbiome (Fuller, 1991, Ouwehand et al., 2002). Fourth, gut mucosal colonization may be highly dependent on the capacity of probiotics to interact with locally-entrenched microbiome niches, which vary in their physiological properties along the GI tract (Donaldson et al., 2016, Mowat and Agace, 2014). Few *in vitro* and mouse-based works have studied probiotic colonization in mucosal GI surfaces (Turroni et al., 2013, Kaushik et al., 2009), while a single human study utilizing culture-based techniques in individuals undergoing surveillance colonoscopy failed to detect efficient probiotics gut colonization (Goossens et al., 2006).

Here, we invasively characterized the homeostatic murine and human gut mucosa-associated microbiome along the GI tract.

We then investigated the effect of prolonged consumption of an 11-strain probiotic preparation versus placebo on the homeostatic mucosal GI niche. To account for inter-individual variability, 15 human volunteers each underwent two invasive colonoscopy and endoscopy procedures, one at baseline and another during consumption of probiotics or placebo, allowing for a person-specific multi-omics assessment of global probiotics effects on the human GI tract. We found that the majority of examined probiotic strains were transiently enriched in feces during the consumption period or shortly thereafter. In inbred WT mice, probiotics gut mucosal colonization was limited by a microbiome-mediated colonization resistance. In humans, marked person-, strain- and gut region-specific mucosal probiotic colonization patterns clustered individuals into those "permissive" or "resistant" to mucosal probiotic colonization. Importantly, these distinct colonization states had differential impacts on probiotics-associated changes in the gut microbial community structure and host transcriptome. Furthermore, the gut mucosal probiotic colonization pattern of a particular individual could be predicted by a combination of unique baseline host and microbiome features.

RESULTS

Murine Stool Microbiome Partially Correlates with the Gut Mucosa Microbiome Configuration

Most evidence supporting beneficial effects of probiotic microorganisms stems from animal and human studies extrapolating from stool microbiome analysis or probiotics quantification to potential impacts of probiotics on host physiology (McNulty et al., 2011, Maldonado-Gómez et al., 2016, Lahti et al., 2013, Hanifi et al., 2015, Wang et al., 2015, Eloe-Fadrosh et al., 2015, Charbonneau et al., 2013, Ferrario et al., 2014). To assess whether stool microbiome represents an accurate marker of upper and lower GI mucosal and luminal microbiome configuration, we performed the MUSPIC1 (MUcosal Search for Probiotic Impact and Colonization 1) study in mice and in humans. We began our investigation by performing a comparative analysis of lumen and mucosa-associated microbiome samples collected from multiple regions of the upper gastrointestinal (UGI) and lower gastrointestinal (LGI) tract of naive male WT mice (Figure S1A, see STAR Methods).

Unweighted UniFrac distances based on 16S rDNA sequencing separated both luminal and mucosal GI samples from stool samples collected from the same mice during the 4 weeks prior to dissection (Figures S1B–S1D). Samples from the LGI were more similar to stool than UGI (Figures S1B–S1D), with the distance to stool being significant for both UGI and LGI (Figure S1C). 100/324 taxa were significantly variable between stool, UGI and LGI (Figure S1D). Among the taxa significantly enriched in the UGI over the LGI of naive mice (Figure S1E) were all common probiotics genera, namely *Lactobacillus, Bifidobacterium, Lactococcus* and *Streptococcus*, as well as *Haemophilus* and *Enterobacteriaceae,* whereas the LGI was enriched with *Prevotella, Bacteroides, Ruminococcus* and *Mucispirillum*.

Similarly, variable OTU representation was noted between the mucosa of the LGI and stool samples (Figure S1F), the LGI lumen
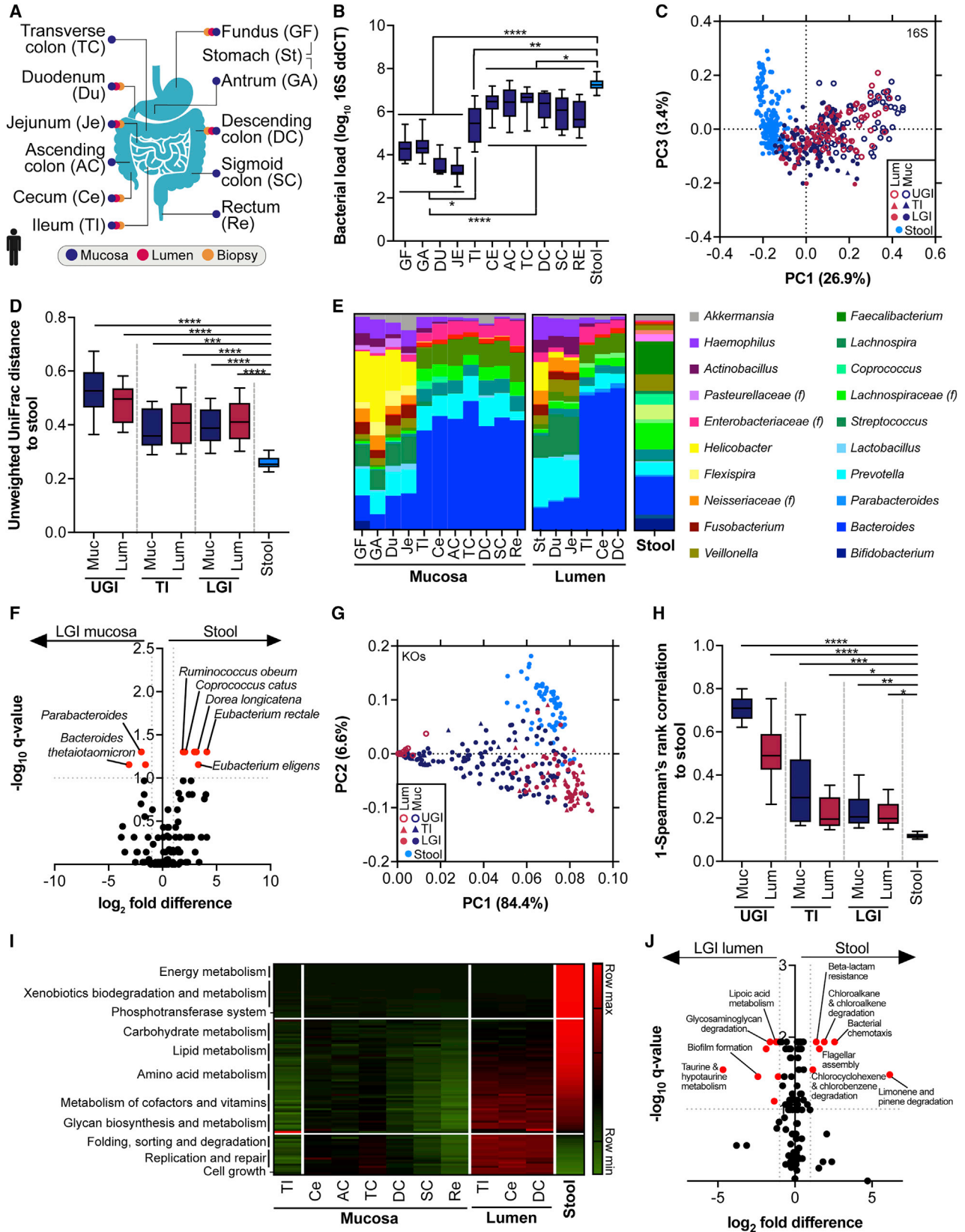
(legend on next page)

and stool (Figure S1G), the lumen and the mucosa of the UGI (Figure S1H) and the lumen and the mucosa of the LGI (Figure S1I). Several taxa were significantly over- or under- represented throughout the GI tract compared to stool (Figure S1J). Both the mucosal and luminal samples of the LGI were richer in the number of species (Figure S1K) and total bacterial load (Figure S1L) compared to the UGI. Collectively, the murine gastrointestinal tract displays a gradient of bacterial richness and a shifting compositional landscape, in which even the most distal lumen samples are significantly different than stool samples, limiting the applicability of stool in fully assessing mucosal GI probiotics colonization.

Human Fecal Microbiome Is a Limited Indicator of Gut Mucosa-Associated Microbiome Composition and Metagenomic Function

Similar to mice, studies on the human GI microbiome rely almost exclusively on stool sampling despite insufficient evidence that these samples accurately reflect the microbial gut mucosal composition and function. We therefore sought to investigate the potential of stool samples as markers for the mucosal GI microbial community by directly sampling throughout the human GI tract. To account for mucosal microbiome-altering impacts of bowel preparation (Drago et al., 2016, O'Brien et al., 2013), we sampled the UGI and LGI tracts of two healthy participants (Table S1) in two consecutive colonoscopies. The first was performed in the absence of any form of bowel preparation, followed by a second procedure 3 weeks later performed using a routine Picolax bowel preparation protocol (Figure S2A, STAR Methods). The terminal ileum (TI) and LGI were affected by bowel preparation more than the UGI (Figure S2B), resulting in separation of the prepped and the non-prepped samples according to 16S rDNA (Unweighted UniFrac, Figure S2C), MetaPhlAn2 (Figure S2D), KEGG orthologous genes (KOs, Figure S2E), and pathways (Figures S2F and S2G), but no significant differences were noted in observed species (Figure S2H) or bacterial load (Figure S2I). These limitations notwithstanding, bowel preparation, greatly facilitating direct gut mucosal sampling at the entirety of the human GI tract, was uniformly applied to all intervention and control cases thereafter.

We began by characterizing the gut microbiome in a cohort of healthy human adults at different bio-geographical regions and directly compared these to stool microbiome configuration of the same individuals. To this aim, 25 healthy participants (Table S1) underwent a compositional and functional microbiome characterization at multiple gut mucosal and luminal regions spanning the LGI, TI and UGI (Figure 1A) via sampling through deep enteroscopy and colonoscopy coupled with stool collection.

Expectedly, microbiome load varied throughout the GI tract. Stool samples harbored the highest bacterial load compared to more proximal GI regions, with a gradient starting from the sparsely populated UGI regions, which were significantly less colonized than the most distal region of the small intestine (TI) and the LGI (Figure 1B). To assess the similarity between stool and GI samples, we calculated unweighted UniFrac distances (Figures 1C and 1D), which demonstrated a significant compositional gradient in which LGI samples were distinct from stool, but more similar to stool than UGI samples. The TI was more similar to stool than more proximal regions of the UGI. A compositional dissimilarity gradient was also observed in shotgun metagenomic sequencing, using MetaPhlAn2 species-based Bray-Curtis dissimilarity indices (Figures S3A and S3B), as reflected by the differences in abundances of the most common genera in each region (Figure 1E). More than 35 taxa were significantly variable between the UGI and LGI (Figure S3C). Several differences between the lumen and the mucosa were observed in both the UGI and LGI (Table S2). Multiple OTUs were significantly over or under-represented in stool compared to the UGI mucosa (31 genera), UGI lumen (34 genera), LGI mucosa (11 genera, and 10 species, Figure 1F), and LGI lumen (15 genera, and 10 species, Table S2).

Given the redundancy in microbial genes and pathways encoded by different microbiome members (Human Microbiome Project Consortium, 2012), and at different bio-geographical locations along the GI tract (Yang et al., 2016), we next set out to determine whether the different regions of the human GI tract display variation in microbial-encoded functions, and whether such variation is reflected in stool. Mapping whole DNA shotgun metagenomic sequencing reads to KOs revealed that, like microbial composition, microbial functions display a dissimilarity gradient throughout the GI tract, starting from stool, to LGI, TI, and UGI samples, with all regions significantly different from stool (Figures 1G–1H, Figure S3D). Mapping KOs to pathways resulted in a similar gradient and significant separation (Figures S3E and S3F). The relative abundance of the 18 most common "housekeeping" pathways in each region was similar between the LGI and stool, but distinct from that of the UGI lumen and mucosa (Figure S3G). In contrast, when comparing the entire set of functionalities represented in each region, 72 pathways were significantly differentially represented between UGI and LGI, while 100

Figure 1. Human Stool Microbiome Is a Limited Indicator of Gut-Associated Microbiome Composition and Metagenomic Function

(A) Anatomical regions sampled during endoscopy procedures.

(B) Bacterial load in mucosal samples quantified by qPCR of the 16S rDNA gene, normalized to a detection threshold of 40. Significance: Kruskal-Wallis & Dunn's.

(C and D) 16S rDNA sequencing-based Unweighted UniFrac distances between stool and the gut microbiome in the upper gastrointestinal tract (UGI), terminal ileum (TI) and lower gastrointestinal (LGI) tract, portrayed in (C) a principal coordinates analysis (PCoA) and (D) quantification of distances to stool. Significance: Kruskal-Wallis & Dunn's.

(E) Relative abundances of the ten most common genera in each anatomical region and stool.

(F) Species significantly variable between the LGI mucosa and stool samples in red (q < 0.1). Significance: Wilcoxon rank sum with FDR correction.

(G and H) Shotgun metagenomic sequencing-based analysis of bacterial KEGG orthologous (KO) genes, (G) PCA of KO relative abundances. (H) Spearman's rank correlation matrices of KOs in stool versus endoscopic samples of luminal and mucosal microbiome. Significance: Kruskal-Wallis & Dunn's.

(I) Groups of KEGG pathways significantly different between stool samples, the LGI lumen or mucosa, or the TI.

(J) Specific pathways significantly variable between stool and the LGI lumen in red (q < 0.1). Significance: Wilcoxon rank sum with FDR correction. Symbols or horizontal lines represent the mean, error bars SEM or 10-90 percentiles. *p < 0.05; **p < 0.01; ***p < 0.001; ****p < 0.0001.

See also Figures S1, S2, and S3.

pathways were significantly differentially represented between stool samples and either the lumen or the mucosa of the LGI (Figure 1I, Table S2). Thus, even the LGI lumen was functionally distinct than stool (Figure 1J). Likewise, host transcriptome obtained from six anatomical locations along the human GI tract (stomach, duodenum, jejunum, terminal ileum, cecum and descending colon) (Figure 1A), featured a region-specific clustering (Figures S3H and S3I). In all, our multi-omics approach demonstrated differential microbiome signatures across GI tract regions and sub-regions in both mice and humans, with even the most distal luminal samples significantly distinct in composition and function from stool. These findings point out the limitations of solely relying on stool as a correlate for intestinal probiotics colonization and impact on the indigenous GI microbiome.

Probiotics Strains Are Present and Viable in the Administered Supplement

To study the effects of commonly consumed probiotics on the mammalian gut, we performed the MUSPIC2 (MUcosal Search for Probiotic Impact and Colonization 2) study in mice and in humans. We focused on a commercial probiotics preparation that included 11 strains belonging to the four major Gram-positive bacterial genera commonly used as empiric probiotics: *Lactobacillus, Bifidobacterium, Lactococcus* and *Streptococcus*. Specifically, the preparation contained the following strains: *Lactobacillus acidophilus* (abbreviated henceforth as LAC), *Lactobacillus casei* (LCA), *Lactobacillus casei* sbsp. *paracasei* (LPA), *Lactobacillus plantarum* (LPL), *Lactobacillus rhamnosus* (LRH), *Bifidobacterium longum* (BLO), *Bifidobacterium bifidum* (BBI), *Bifidobacterium breve* (BBR), *Bifidobacterium longum* sbsp. *infantis* (BIN), *Lactococcus lactis* (LLA), and *Streptococcus thermophilus* (STH). In order to determine the presence and viability of these 11 strains in the supplement, we first analyzed 16S rDNA amplicons obtained from the supplement pill with and without culturing. All four genera (and no others), but only 4/11 species (BBI, BLO, LAC, LCA), were identified by 16S rDNA analysis in the pill and in colonies resulting from plating of the pill on different solid media with or without prior overnight culture in liquid medium (Figure S4A). As this result might stem from insufficient sensitivity of 16S rDNA sequencing rather than the actual absence of the strains, we employed shotgun metagenomic sequencing-based MetaPhlAn2 analysis that indeed identified 10/11 species, excluding BIN (Figure S4B). MetaPhlAn2 analysis of a pure culture of BIN indicated that it is identified at the species level as *B. longum*. As an additional validation of probiotics strains presence, genomes for nine of the 11 probiotic strains were recovered at >93% completeness and <4% contamination from metagenomics samples of the probiotics pill using reference-based and mini-assembly approaches (Sharon et al., 2013). For one of the species (*B. longum*), only part of the genome was recovered due to strain heterogeneity between BLO and BIN. As the abundance of several strains noted using MetaPhlAn2 was close to the detection threshold, we utilized species-specific qPCR primers and validated them on DNA obtained from pure cultures. All targets were identified in their corresponding templates at CT (cycle threshold) values significantly lower than those observed in mismatched target-template pairs, and did not pass the detection threshold (40)

for most mismatched pairs (Figure S4C), resulting in a near-perfect area under the receiver-operator curve (ROC AUC) of 1 and p < 0.0001 (Figure S4D). qPCR amplification identified all 11 species in DNA purified independently from six different batches of pills with high reproducibility, though only 6/11 strains (BLO, LAC, LLA, LPL, LRH and STH) were found above the detection threshold after two subsequent cultures in liquid and solid BHI (Figure S4E). To assess viability *in vivo*, we inoculated germ-free (GF) mice with the probiotics pill content and quantified the 11 species in stool samples collected 5 days post-inoculation, with all strains but BIN being cultivable (Figure S4F). Live count of colonies grown from the pill on BHI resulted in 5 × 10^9 CFU, in line with the manufacturer's statement. The abundances of most probiotics species were unchanged following bowel preparation (with the exception of BIN, BLO and STH), resulting in a significant positive correlation between per-tissue and individual levels of the probiotics species with or without bowel preparation (Spearman r = 0.77, p < 0.0001, Figure S2J). Together, a combined culture-dependent and -independent approach utilizing 16S rDNA and shotgun metagenomic sequencing and qPCR validation readily identified all probiotics strains with high specificity, and all but BIN were proven to be viable under the aforementioned experimental conditions.

Murine Microbiome-Driven Colonization Resistance Limits Probiotics Mucosal Colonization and Impact on the Indigenous Microbiome

To assess the degree of murine GI colonization by probiotics, we administered the contents of one pill daily by oral gavage to adult male specific-pathogen-free (SPF) WT mice, with an additional group of untreated mice serving as controls (Figure 2A). Stool samples were analyzed at the indicated time points, followed by a dissection of the GI tract (Figure S1A) on day 28 of supplementation. Highly specific qPCR amplification demonstrated significant stool shedding of BLO and STH in the probiotics group relative to baseline and no significant shedding in the control (Figure 2B). When all the probiotic targets were considered together, an average 8.6-fold fecal enrichment compared to baseline was observed in the treated group, resulting in significant differences between probiotics and control after 28 days of supplementation (15-fold, Figure 2C) and a significantly higher area under the curve.

16S rDNA-based compositional analysis of luminal and mucosal samples collected throughout the GI tract did not indicate any significant differences between the probiotics and control groups in any region for any of the four probiotics genera (Figure S4G). Species-specific qPCR also demonstrated minimal differences between the probiotics and the control groups. The only significant difference in the mucosa was in cecal levels of STH (Figure 2D). Significant differences in the lumen were restricted to the stomach and the LGI and were most pronounced in the distal colon (Figure 2D).

We hypothesized that this limited colonization of probiotics at the murine gut mucosal regions may result from colonization resistance of the microbiome to the supplemented strains. To address this possibility, we inoculated GF mice with an identical probiotic preparation by oral gavage and housed them in sterile isocages (Hecht et al., 2014) for 14 days before dissecting their GI tract (Figure 2E) and utilized qPCR to directly compare the GF-Probiotics,
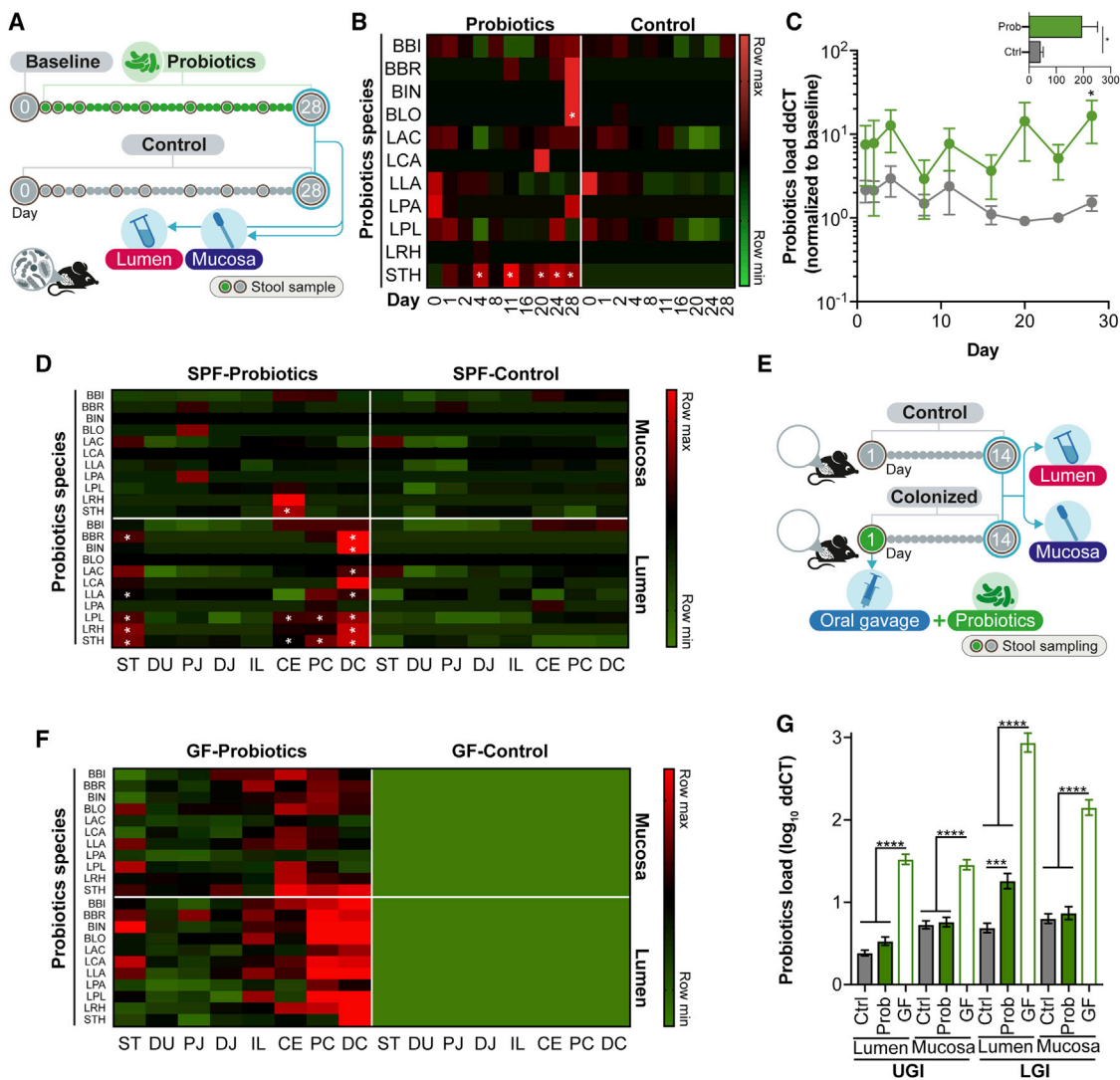
Figure 2. Colonization Resistance to Probiotics Is Driven by the Murine Gut Microbiome

Specific-pathogen-free (SPF) mice were gavaged daily with probiotics (Prob, n = 10) or remained untreated (Ctrl, n = 10) for 28 days.

(A) Experimental design in SPF mice.

(B) Quantification of specific probiotics species in stool by qPCR. *, any p < 0.05 for clarity, Two-Way ANOVA & Dunnett compared to baseline.

(C) Aggregated qPCR-based quantification of all probiotics targets in stool samples, normalized to baseline. *p < 0.05, Two-Way ANOVA and Sidak. Inset: area under incremental bacterial load curve. *p < 0.05, Mann-Whitney.

(D) Species-specific qPCR of probiotics in mucosal and luminal samples throughout the murine GI tract on day 28. *, any p < 0.05 for clarity, Two-Way ANOVA & Dunnett versus control.

(E) Experimental outline in GF mice.

(F) Same as (D), but in GF mice, row min/max scale matches with (D).

(G) qPCR-based enumeration of pooled probiotics targets in luminal and mucosal subregions of SPF and GF GI tracts, normalized to a detection threshold CT of 40. ***p < 0.001; ****p < 0.0001, Kruskal-Wallis test and Dunn's. Symbols and horizontal lines represent the mean, error bars SEM. The experiment was repeated 3 times.

See also Figure S4.

SPF-Probiotics, GF-Control and SPF-Control mouse groups. No amplification was detected by any of the primer sets in GI tissues from GF-Control mice (Figure 2F). In contrast, significant colonization of the probiotic strains was observed in GF-Probiotics mice compared to either of the SPF groups (Figures 2F and 2G). As such, gut probiotics colonization in supplemented GF mice

increased by 10-fold, 5-fold, 20-fold, and 50-fold in the UGI lumen, UGI mucosa, LGI mucosa and LGI lumen, respectively, as compared to probiotics-treated SPF mice. In comparison to this striking colonization in GF mice, aggregated fold increase of probiotics was only significant in the LGI lumen of SPF mice as compared to non-treated mice (3.7-fold difference, Figure 2G).
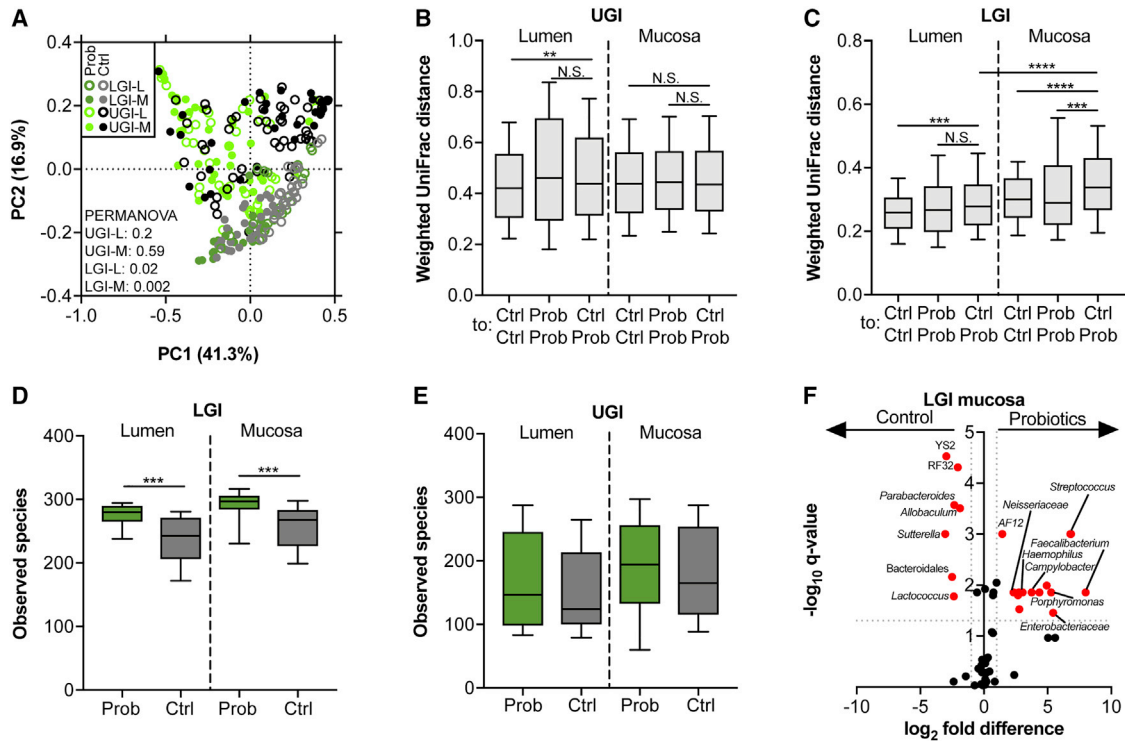
Figure 3. Probiotics Impacts on the Murine Gastrointestinal Microbiome

Microbiota alterations were assessed following probiotics administration in GI mucosal and luminal samples.

(A–C) PCoA of weighted UniFrac distances between probiotics-administered mice or controls in GI tract tissues and quantification in the (B) UGI or (C) LGI. Significance: PERMANOVA for (A), Kruskal-Wallis & Dunn's for (B and C).

(D and E) Observed species in the (D) LGI or the (E) UGI. Significance: Mann-Whitney.

(F) Taxa significantly different between control and probiotics in the LGI mucosa in red (q < 0.05). Significance: FDR-corrected Mann-Whitney. Horizontal lines represent the mean, error bars 10-90 percentiles. **p < 0.01; ***p < 0.001; ****p < 0.0001. Lum, lumen; Muc, mucosa; Ctrl, control; Prob, probiotics; UGI, upper gastrointestinal tract; LGI, lower gastrointestinal tract.

See also Figure S4.

We next assessed the impact of the above murine low-level probiotic colonization on the indigenous fecal and mucosal microbiome configuration. Both unweighted and weighted UniFrac distances of fecal samples (rarefied to 20,000 reads) to baseline indicated no differences between the probiotics and control groups (Unweighted PERMANOVA p = 0.35, weighted p = 0.75), and there were no significant differences in fecal alpha diversity in the treated group, resulting in only five taxa that were significantly different between probiotics and control mice on the last day of supplementation (Table S3).

While no consistent probiotics-induced alterations of the UGI luminal and mucosal microbiome were observed (Figures 3A and 3B), a significant shift was noted in the LGI microbiome, which was more pronounced in the mucosa compared to the lumen (Figure 3C). These changes were accompanied with an increase in observed species both in the LGI lumen and mucosa (Figure 3D), but not the UGI (Figure 3E) of probiotic-administered mice. None of the aforementioned significant differences were merely due to the presence of the probiotics genera, as removal of the relevant genera and reanalysis after rarefaction to 20,000 reads (stool) or 5,000 reads (lumen and mucosa) did not affect the significantly higher alpha diversity in the LGI (Figure S4H),

as well as the weighted UniFrac distances in the UGI (PERMANOVA for lumen p = 0.1; mucosa p = 0.29, Figure S4I) or the LGI (PERMANOVA for lumen p = 0.02; mucosa p = 0.001, Figure S4J). Collectively, 21 OTUS were differentially represented between probiotics and control in the LGI mucosa (Figure 3F). Interestingly, 10/14 OTUs that bloomed in the LGI mucosa of the probiotics group are characteristic of the oral cavity, the stomach, or both, as reported both by our mouse and human homeostatic analysis (Figure S1E, Table S2, Figure S3C) and by others (Human Microbiome Project Consortium, 2012, Bik et al., 2006).

Taken together, these findings suggest that despite daily administration, human-targeted probiotics feature low-level murine mucosal colonization, mediated by resistance exerted by the indigenous murine gut microbiome. Even at these low colonization levels, probiotics induced modulation of the LGI mucosal microbiome, which was not observed in stool samples.

Inter-individual Differences in Probiotics Colonization of the Human GI Tract

In contrast to inbred mice, humans display considerable person-to-person variation in gut microbiome composition, which
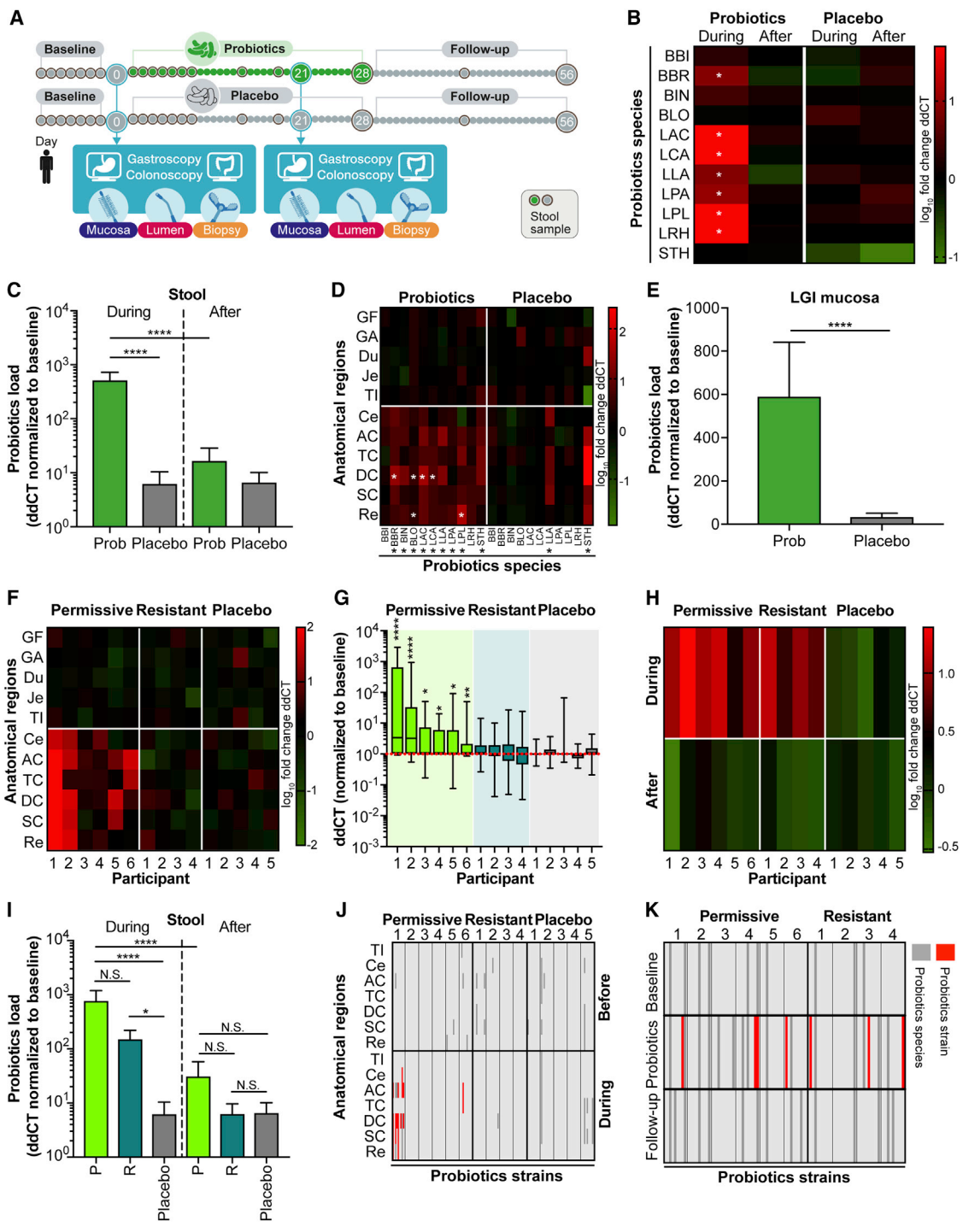
Figure 4. Global and Individualized Probiotics Colonization Patterns in the Human GI Tract

Human participants were treated with probiotics pills or placebo bi-daily for a period of 28 days and were further followed for 1 month.

(A) Experimental outline in humans.

(B) qPCR of probiotics species fecal shedding in supplemented individuals or placebo on day 19 of consumption and 1 month after probiotics cessation, normalized to baseline. *, any p < 0.05 for clarity, Two-Way ANOVA & Dunnett.

(C) Aggregated probiotics load in feces. ****p < 0.0001, Kruskal-Wallis & Dunn's.

(D) Same as (B), but in the LGI and UGI mucosa at day 21 normalized to baseline. Two-Way ANOVA for species, with Dunnett per species per region.

(E) Aggregated probiotics load in the LGI mucosa normalized to baseline. ****p < 0.0001, Mann-Whitney and permutation tests.

(legend continued on next page)

may be more permissive to colonization with exogenous probiotics bacteria. To test this, we conducted a placebo-controlled trial, in which 15 healthy volunteers (STAR Methods, Table S1) received either an identical 11-strain probiotics preparation or a cellulose placebo bi-daily for a 4-week period. Stool was sampled at multiple time points before, during, and after the administration of probiotics or placebo; colonoscopy and deep enteroscopy were performed prior to intervention and 3 weeks after the initiation of probiotics or placebo consumption in all participants (Figure 4A). 16S rDNA analysis could not detect significant enrichment of *Lactobacillus* (Figure S5A), *Bifidobacterium* (Figure S5B), or *Streptococcus* (Figure S5C) in stool samples during or after the supplementation period compared to baseline, whereas a 2.4-fold increase was observed for *Lactococcus* (Figure S5D). Likewise, no significant differences were found when comparing the relative abundances of the probiotics genera in the luminal and mucosal samples of the supplemented group either to their own baseline or to the placebo group (Figures S5E and S5F). The more sensitive species-specific qPCR demonstrated significant shedding of 7/11 strains during consumption (BBR, LAC, LCA, LLA, LPA, LPL and LRH, Figure 4B). Aggregated probiotics fold difference significantly dropped to baseline after probiotics cessation (Figures 4B and 4C). There were no significant differences in the placebo group compared to baseline for any of the species (Figures 4B and 4C). Species-based MetaPhlAn2 fold change analysis mirrored the qPCR findings, though none of the species reached statistical significance (Figure S5G). With the exception of a significant increase of LAC in the TI lumen, none of the probiotics species were significantly increased in any of the luminal samples compared to either baseline or placebo (Figure S5H). In contrast, qPCR demonstrated that 9/11 probiotics species were significantly enriched in the mucosa of the supplemented group compared to baseline, which was more pronounced in the LGI, especially in the AC and DC (Figure 4D). LRH was also significant when only the LGI was analyzed (Figure 4D). As opposed to the ten species that bloomed in the LGI of the treated group, only two species (LLA and STH) significantly bloomed in the placebo group compared to baseline. Nonetheless, the aggregated probiotics fold change was significantly higher in the treated group (Figure 4E). MetaPhlAn2 validated this observation (Figures S5I and S5J).

Surprisingly, when each participant was analyzed independently compared to their own baseline, the gastrointestinal mucosal load of probiotics strains considerably varied, with both qPCR (Figure 4F, Figure S6A) and MetaPhlAn2 (Figure S6B) analyses pointing out to some individuals as featuring significant

gut mucosal association of probiotics as compared to others. Both MetaPhlAn2 and qPCR identified two participants (Permissive 1 & 2, 10,000 permutations p = 0.003 and p < 0.0001 respectively) as very significantly colonizing (Figures 4F–4G, Figures S6A and S6B), and qPCR also identified four more participants (Permissive 3-6 p = 0.034, p = 0.026, p = 0.03 and p = 0.002, Figure 4G) as probiotics colonizers. We defined individuals with a significant elevation in the absolute abundance of probiotic strains in their GI mucosa (as determined by Mann-Whitney test and validated by 10,000 permutations) as "permissive" (Figures 4F–4G, Figure S6A). Of note, even among the permissive, some (1 and 2) were more colonized than others (3–6), with participant 1 featuring the highest probiotics colonization, followed by participant 2, then by the other four permissive individuals. Individuals with no significant colonization were termed "resistant."

Importantly, both the relative (Figure S6C) and absolute (Figures 4H–4I, Figure S6D) abundance of probiotics strains in stools did not reflect this personalized mucosal colonization trait, with both permissive and resistant individuals featuring significant and comparable stool shedding during consumption (Permissive 1–4 and 6, and resistant 1 and 3, Figures 4H–4I, Figures S6C and S6D), with even resistant individuals shedding significantly more probiotics in stool as compared to the placebo group (Figure 4I). Once probiotic supplementation ceased, neither permissive nor resistant individuals featured a persistently significant stool shedding compared to placebo (Figure 4I). Moreover, strain-level analysis indicated that probiotic species found in stool and mucosal samples during the intervention period were, indeed, identical to the strains present in the administered pill, but were distinct from the ones excreted in stool at baseline or the follow-up period (Figures 4J and 4K). Thus, and in contrast to previous stool-focused studies (Maldonado-Gómez et al., 2016, Frese et al., 2012), we found shedding of probiotics species in stool to be non-indicative of person-specific gut mucosal colonization. As validation, four additional participants consumed probiotics according to the same protocol, collected stool samples and underwent a single colonoscopy after 21 days of probiotic supplementation. Like the main MUSPIC2 cohort, qPCR-based quantification of probiotics species in the GI mucosa of these participants demonstrated marked inter-individual colonization differences (Figures S7A and S7B), which were indistinguishable by probiotic assessment in stool (Figures S7C and S7D). Taken together, these findings point out that human consumption of the examined 11 probiotic strains results in universal shedding in stool but with highly individualized LGI mucosa colonization patterns.

(F and G) qPCR-based quantification of mucosal colonization with the 11 probiotics strains pooled for each participant in (F) each anatomical region or (G) aggregated, values during probiotics/placebo normalized to each individual baseline in each region. *p < 0.05; **p < 0.01; ****p < 0.0001, Mann-Whitney and permutation tests.

(H) Same as (B), but per participant.

(I) Same as (C), but aggregated per group of individuals. *p < 0.05; ****p < 0.0001, Mann-Whitney.

(J and K) Probiotics strain quantification based on mapping of metagenomic sequences to unique genes, which correspond to the strains found in the probiotics pill in (J) the GI tract or (K) stool samples. P, permissive; R, resistant. N.S., non-significant. LGI, lower gastrointestinal tract. Prob, probiotics. Horizontal lines represent the mean, error bars SEM or 10-90 percentiles.

See also Figures S5, S6, and S7.
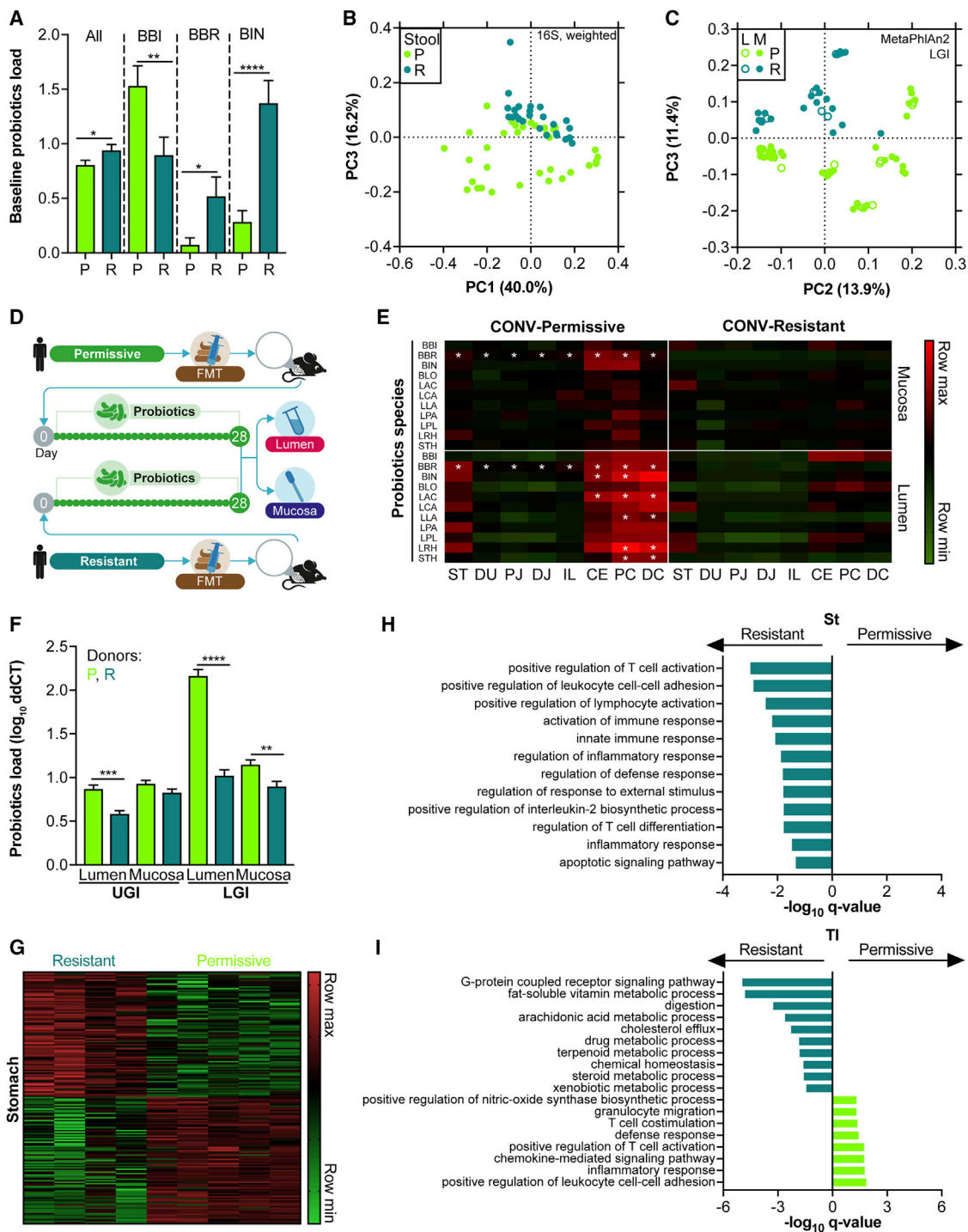
Figure 5. Microbiome and Host Factors Associate with Probiotic Colonization Pattern

(A) Aggregated probiotics load and specific species significantly distinct at baseline between permissive (P) and resistant (R) individuals in the LGI mucosa. *p < 0.05; **p < 0.01; ****p < 0.0001, Mann-Whitney.

(B) PCoA of 16S-based weighted UniFrac distances separating stool microbiome composition of permissive from resistant individuals prior to probiotics supplementation. Mann-Whitney on the difference between inter- and intra-group distances p < 0.0001.

(C) Same as (B) by MetaPhlAn2-based PCA in the LGI (p < 0.0001).

(D) Experimental validation of a causative role for the microbiome in resistance to probiotics; pre-supplementation fecal samples from 3 permissive (P1, n = 7 mice; P2, n = 6; P3, n = 7) or resistant (R1, n = 5; R3, n = 9) individuals were used to conventionalize (CONV) 5 groups of GF mice, followed by daily gavage with probiotics and GI dissection after 28 days.

(legend continued on next page)

Baseline Personalized Host and Mucosal Microbiome Features Are Associated with Probiotics Persistence

We next set out to identify factors that may dictate or mark the extent to which probiotics colonize the human GI mucosa. Interestingly, we observed a significant inverse correlation between initial levels of a given probiotics species in a given GI region and its fold change, i.e., low abundant species were more likely to expand than those already present in high loads (Figure S7E). When taken together, permissive individuals had significantly lower baseline levels of the probiotics strains in the LGI mucosa (Figure 5A), but not in stools. When each strain was compared individually, both BBR and BIN were significantly lower in permissive individuals (Figure 5A), and LAC was marginally but non-significantly lower in the permissive subset (p = 0.056). In contrast, BBI, the only strain that did not significantly colonize the LGI mucosa (Figure 4D), was higher in permissive individuals at baseline (Figure 5A). In addition, permissive and resistant individuals clustered separately at baseline according to stool microbiome composition (Figure 5B, Figures S7F and S7G) and function (KOs, Figure S7H; Pathways, Figure S7I), as well as LGI composition (Figure S7J; MetaPhlAn2, Figure 5C).

To determine whether these compositional and functional microbiome differences between permissive and resistant individuals impact colonization capacity of probiotics, we conventionalized five groups of GF mice with baseline stool samples from either permissive or resistant individuals. Probiotics were administered to the conventionalized mice daily by oral gavage for 4 weeks, after which the load of probiotics in the GI tract lumen and mucosa was quantified by qPCR (Figure 5D). Both the LGI lumen and mucosa, as well as the UGI lumen of mice conventionalized with "permissive" microbiomes, were significantly more colonized compared to those of mice conventionalized with "resistant" individuals' microbiome (Figures 5E and 5F). Thus, as observed in mice (Figure 2), the resident microbiome contributes to person-specific permissiveness or resistance to colonization of the examined exogenous probiotics.

In order to identify host factors that may affect permissiveness or resistance to probiotics colonization, we performed a global gene expression analysis through RNA sequencing of transcripts collected from stomach, duodenum, jejunum, terminal ileum, and descending colon biopsies before probiotics supplementation. Two clusters of genes that were higher in permissive versus resistant and vice versa were visible in the stomach (Figure 5G). Interestingly, host pathways significantly enriched in resistant compared with permissive were related to both adaptive and innate immune responses, inflammation and T cells activation and differentiation (Figure 5H). In contrast to the stomach, immune-related pathways were significantly enriched in the ilea of permissive versus resistant individuals, whereas pathways enriched in resistant individuals included ones related to digestion, metabolism, and xenobiotics metabolic processes (Figure 5I). To

conclude, both indigenous microbiome and host factors are differentially expressed in individuals permissive and resistant to colonization of the examined probiotics, even prior to exposure to probiotics. These host and microbiome factors may contribute to a differential colonization susceptibility to probiotics, potentially through competitive exclusion of related species and site-specific immune responses.

Probiotics Differentially Affect Permissive and Resistant Human Individuals

Finally, as the effect of probiotics on the human GI microbiome remains inconclusive (Kristensen et al., 2016), we sought to determine probiotic impact on microbiome composition and function and the host transcriptome, and whether these follow personalized patterns. We compared stool samples collected during and after probiotics or placebo supplementation to each participant's baseline, using 16S rDNA and MetaPhlAn2 compositional analysis, and shotgun metagenomic functional mapping to KOs and KEGG pathways.

Stool microbiome composition was distinct from baseline during the probiotic exposure period (Figure 6A, Figure S8A). There were no significant differences in the microbiota composition of the placebo group, resulting in a significantly higher area under the distance to baseline curve in the treated group (Figure 6A). Nonetheless, only a few genera (Figure 6B) and species (Figure 6C) bloomed or diminished in stools of the probiotics group, though they remained elevated 1 month following cessation. Even fewer species in stool were significantly different between baseline and the last day of probiotics supplementation (Table S3) or 1 month following probiotics cessation (Table S3). Multiple KOs (Figure 6D) which were mapped to eight pathways (Figure 6E) were altered by probiotics but not by placebo, though this did not result in significant global differences in distances to baseline based on KOs (Figure S8B) or pathways (Figure S8C). The number of observed species in stool was also not significantly altered by probiotics (Figure S8D).

A similar region-specific comparison of compositional and functional microbiome differences induced by the probiotics and placebo groups in luminal and mucosal samples, using all four microbiome readouts (16S rDNA, MetaPhlan2, KOs, and pathways), resulted in not even a single indigenous microbiome feature that was significantly different between the groups. We therefore clustered luminal or mucosal samples to UGI and LGI and utilized a permutations-based test for all the modalities. In the UGI, weighted UniFrac separated the lumen of probiotics from that of placebo (p = 0.04, Figure 6F), although significance of this separation was lost when the probiotics genera were omitted from the analysis (p = 0.071). The UGI mucosa did not differ between the probiotics to placebo groups according to weighted UniFrac (p = 0.35, Figure 6F), and no other significant differences were detected in the UGI by MetaPhlan2 (lumen

---

(E and F) Probiotics load normalized to a detection threshold of 40 (E) per species per anatomical region. *, any p < 0.05 for clarity, Two-Way ANOVA & Sidak.

(F) Aggregated probiotics in the GI of conventionalized germ-free mice. **p < 0.01; ***p < 0.001; ****p < 0.0001, Mann-Whitney.

(G) Genes that differ in abundance between permissive and resistant individuals in the stomach prior to probiotics supplementation.

(H) Pathways that are significantly enriched after FDR-correction in resistant stomachs at baseline. No pathways were significantly enriched in permissive.

(I) Same as (H), but in the terminal ileum with both groups showing discriminating pathways. Horizontal lines represent the mean, error bars SEM.

See also Figure S7.
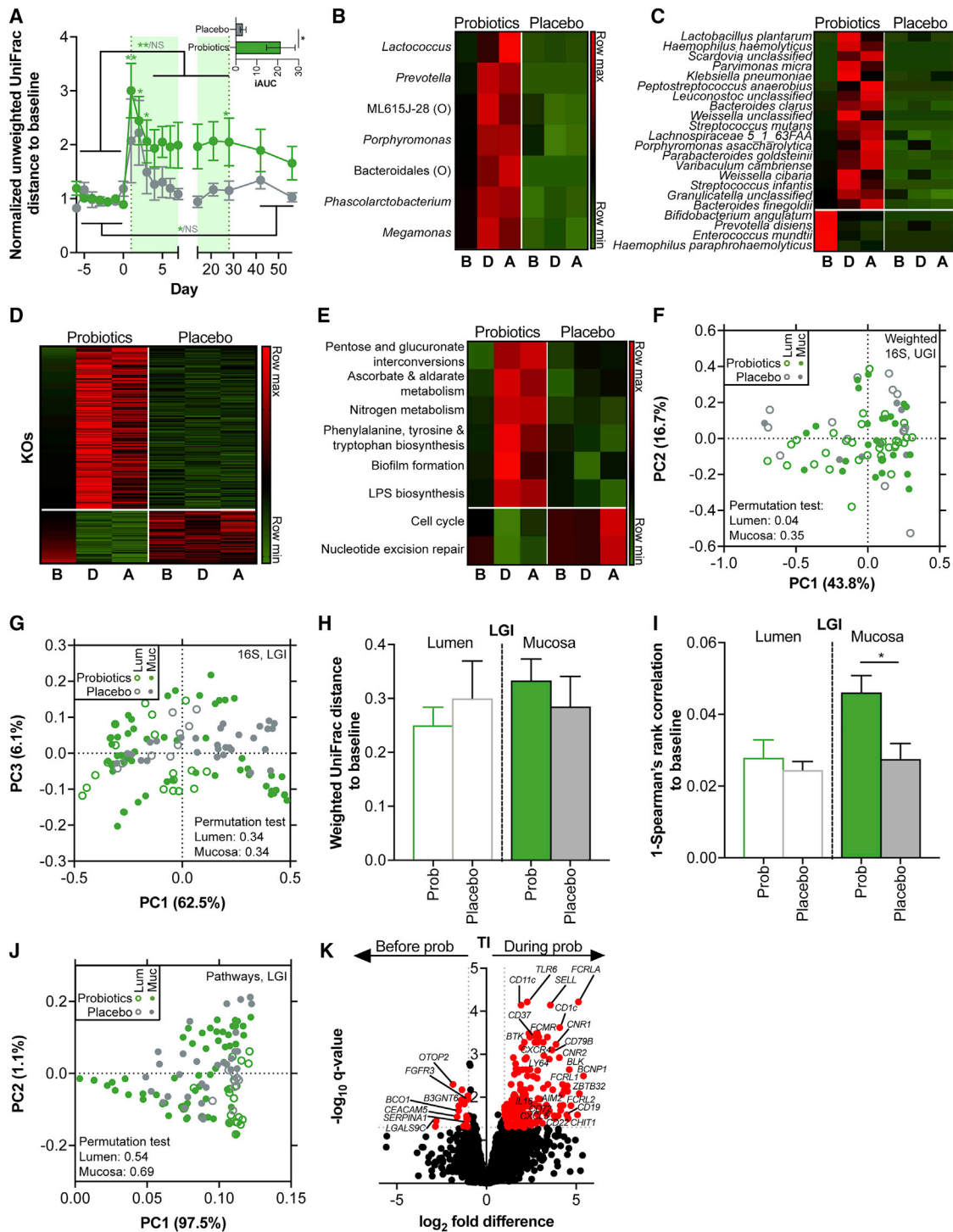
Figure 6. Effects of Probiotics on the Human Gut Microbiome and Host Transcriptome

(A) Unweighted UniFrac distances between 16S rDNA sequencing-based taxa abundances of stool samples collected throughout the study normalized to their respective baseline samples, in the probiotics and placebo groups. Asterisks on horizontal lines compare periods according to a paired Friedman's test & Dunn's, excluding days 1–3; green asterisks on symbols according to Two-Way ANOVA & Dunnett to probiotics baseline. Inset, incremental area under the distance curves during supplementation, from baseline and excluding days 1–3. Significance: Mann-Whitney.

(B) 16S-based genera that bloomed or diminished in probiotics, but not in placebo.

(C–E) Same as (B), but for (C) MetaPhlAn2-based species, (D) KOs and (E) KOs mapped to KEGG pathways.

p = 0.75, mucosa p = 0.11), KOs (lumen p = 0.6, mucosa p = 0.5), or pathways (lumen p = 0.6, mucosa p = 0.37). Likewise, weighted UniFrac did not distinguish between the groups after 1 month of consumption in the LGI lumen (p = 0.34, Figure 6G) or mucosa (p = 0.34, Figure 6G), and both groups changed to the same extent compared to baseline (lumen p = 0.68, mucosa p = 0.44, Figure 6H). MetaPhlan2 reflected the absence of compositional differences (Figures S8E and S8F). Compared to baseline, more microbiome pathways were altered in the LGI mucosa of probiotics than in placebo (p = 0.019, Figure 6I). Nonetheless, neither KOs (lumen p = 0.62, mucosa p = 0.66, Figure S8G) nor pathways (lumen p = 0.54, mucosa p = 0.69, Figure 6J) separated between the groups after 1 month of consumption. To conclude, when all probiotics consumers are compared either to placebo or to their own per-probiotic baseline, minimal significant compositional changes are observed in stool samples. Similarly, in the GI tract, no probiotic effect is noted on the indigenous UGI and LGI microbiome. Nonetheless, when all probiotics-consumers were considered together, probiotics consumption led to transcriptional changes in the ileum, with 19 downregulated and 194 upregulated genes noted, many of which related to the immune system including B cells (Figure 6K).

We next hypothesized that differential probiotics colonization patterns noted in subsets of participants may result in differential effects on the microbiome and host transcriptome, which can be obscured when all individuals are considered together. Indeed, during probiotic supplementation, compositional changes were pronounced in stools of permissive more than in resistant participants, as evident by higher distances to baseline (Figure 7A, Figure S8H). Some taxa (e.g. Haemophilus, Enterococcus faecium), mostly characteristic of the UGI (Figure 1, Table S2, Figure S3C), were higher in permissive at baseline and were reduced to levels comparable to resistant following probiotics, while others (e.g., Prevotella and Sutterella wadsworthensis) bloomed only in permissive participants (Figure 7B, Figure S8I). Stool microbiome functionality recapitulated the differences noted between the permissive and resistant groups, with changes from baseline more evident in permissive participants (Figures S8J and S8K, Figures 7C and 7D). The initial compositional differences in the LGI mucosal microbiome between permissive and resistant participants were maintained upon probiotics supplementation (Figures 7E and 7F), with a reduction of UGI-characteristic species, coupled with multiple blooming taxa, observed in permissive participants (Figure 7G). Interestingly, probiotic supplementation was associated with a decrease in observed species (Figure 7H) but an increased total bacterial load in stool (Figure 7I) in permissive as compared to resistant individuals. Total bacterial load remained higher than baseline in permissive participants even 1 month following probiotics cessation, while it readily returned

to baseline in resistant participants (Figure 7I), and remained stable throughout in placebo controls. Like in stool, bacterial load was significantly elevated in the LGI mucosa of permissive participants, compared to either resistant participants or placebo controls (Figure 7J).

Probiotics also differentially affected the host GI transcriptome. Following initiation of probiotic consumption, all the previously significant baseline ileum host pathways that distinguished permissive from resistant individuals (Figure 6K) were ablated. Instead, following probiotics exposure, the cecum emerged as a distinguishing region between the permissive and resistant groups (Figure 7K), with ceca of permissive individuals being enriched for pathways related to dendritic cells, antigen presentation, and ion transport, while ceca of resistant individuals featuring enrichment of multiple pathways associated with responses to exogenous stimuli, innate immune activation, anti-bacterial defense, and specifically against Gram-positive bacteria (potentially related to all probiotics species assessed in this study being Gram-positive). Additionally, following probiotics consumption, descending colons of permissive individuals became enriched for three pathways associated with humoral immune response and cytokine-mediated signaling, while no pathways were enriched in colons of resistant individuals (Figure S8L). Taken together, the examined probiotics featured a person-specific differential effect on GI microbiome composition and function and the host GI transcriptome, whose potential mechanisms of health impacts on the responding hosts merit further studies.

DISCUSSION

In this work, we profiled the homeostatic mucosal, luminal, and fecal microbiome along the entirety of the gastrointestinal tract of mice and humans. We demonstrated that solely relying on stool sampling as a proxy of mucosal GI composition and function may yield limited conclusions. In contrast, direct gastrointestinal sampling in mice and humans, before and during an 11-strain probiotic consumption, indicated that the examined probiotics readily passed through the gastrointestinal tract into stool, but encountered along the way a near-universal microbiome-mediated mucosal colonization resistance (in mice) or a person-, strain- and region- specific colonization resistance (in humans), the level of which significantly impacted probiotics effects on the indigenous mucosal microbiome composition, function, and host gene expression profile. In humans, individualized gut mucosal colonization capacity correlated with baseline host transcriptional and microbiome characteristics, but not with stool levels of probiotics during consumption.

Our results highlight several important concepts. First, we expand the scope of description of the human microbiome

(F–H) 16S-based weighted UniFrac distance between probiotics and placebo supplemented individuals after 21 days in the (F) UGI or the (G and H) LGI. Significance: permutation tests for (F) and (G), Mann-Whitney test for (H).
(I) KEGG pathways-based 1-Spearman's correlation to baseline in probiotics and placebo LGI mucosa. Significance: Mann-Whitney test.
(J) PCA based on KEGG pathways in the LGI mucosa of probiotics and placebo on day 21. Significance: permutation test.
(K) Genes significantly altered in expression levels in the ileum of probiotics consuming individuals between day 21 and baseline in red (q < 0.05), FDR corrected. B, before supplementation; D, during; A, after. P, probiotics. O, indicates an OTU belonging to that order. Horizontal lines represent the mean, error bars SEM. *p < 0.05; **p < 0.01. Permutation test (100,000 permutations, panels F, G and J), Mann Whitney (panels H-I). See also Figure S8.
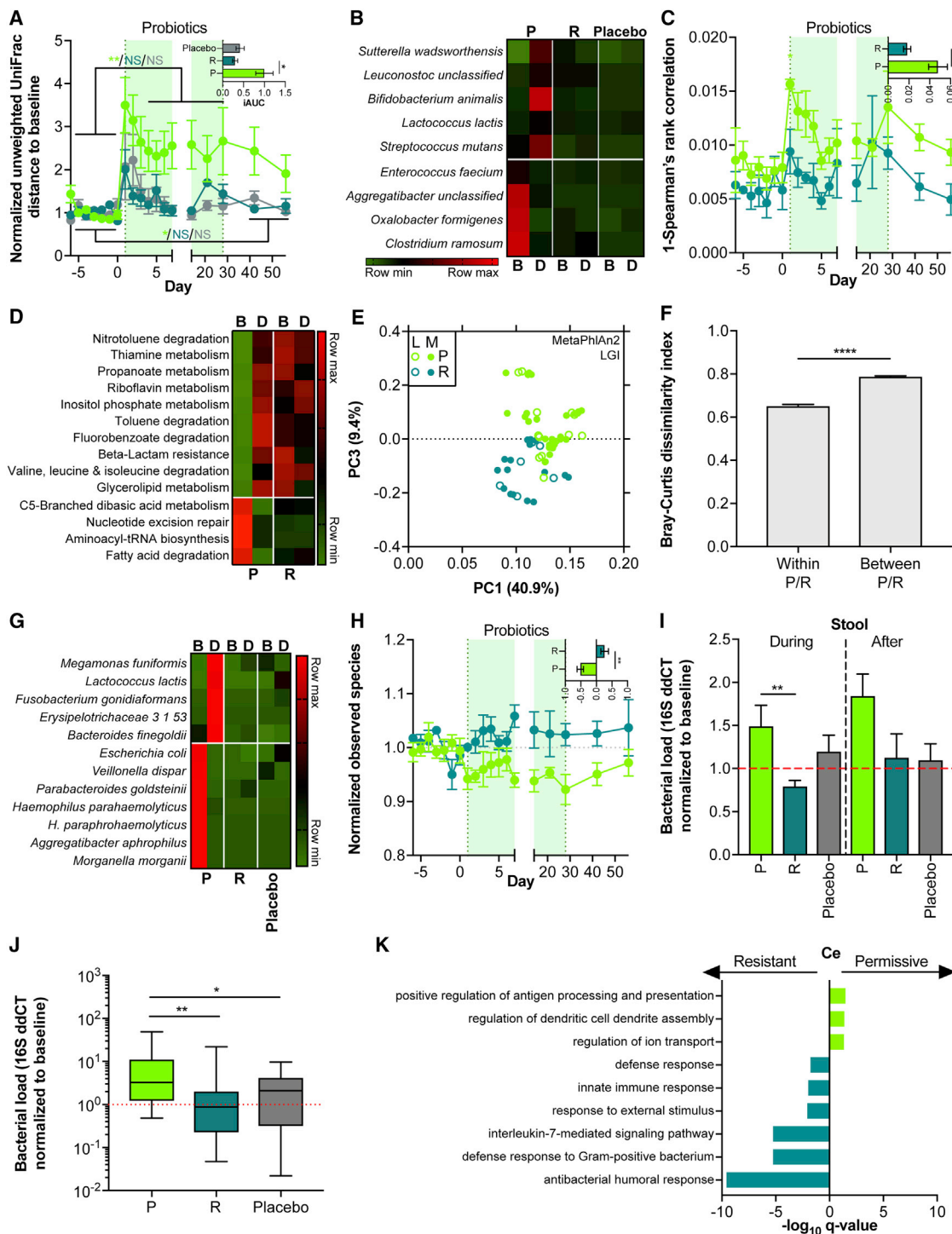
Figure 7. Probiotics Differentially Affect the Stool and Gut Mucosa in Permissive and Resistant Individuals

(A) 16S-based distances to baseline in stools of permissive (P), resistant (R), and placebo-consuming individuals, normalized to baseline stool samples. Asterisks on horizontal lines compare periods according to a paired Friedman's test & Dunn's, excluding days 1-3. Inset: area under the distance to baseline curve during supplementation, from baseline and excluding days 1-3. Significance: Mann-Whitney.

(B) Species that changed in relative abundance in permissive individuals during (D) probiotics consumption compared to baseline (B) but not in resistant or placebo.

(C and D) Same as A-B, but with KEGG pathways and 1-Spearman's correlation.

(legend continued on next page)

bio-geographical compositional and functional landscape (Donaldson et al., 2016, Mowat and Agace, 2014), and indicate that extrapolation from stool microbiome communities to those of specific GI mucosal and luminal niches may lead, in some cases, to inaccurate conclusions. By directly comparing the stool and mucosal presence of 11 probiotic strains of the most commonly used probiotic genera, we conclude that probiotic strain expansion in stool, highlighted by most previous studies to be a sign of probiotics efficacy (Del Piano et al., 2010, Jacobsen et al., 1999, Tannock et al., 2000), cannot distinguish between true probiotic-permissive and resistant individuals, in which probiotics in stool represent a transient "washout" of non-colonizing strains passing throughout the GI lumen without significantly adhering to the host mucosal layer. More generally, these results call for greater use of gut mucosal sampling in studying host-microbiome interactions, while highlighting the need for development of better predictive models inferring gut microbiome mucosal composition and function from fecal configurations.

Second, the marked and person-specific mucosal colonization resistance to probiotics noted in our study may explain the high variability in probiotics effects on the host or its microbiome noted in previous works (Kristensen et al., 2016). One important feature shown in our studies (Suez, et al., 2018) to play a central role in impacting individualized probiotic mucosal colonization is the indigenous gut microbiome, which may drive the observed person-, strain-, and region-specific colonization resistance patterns to probiotics, as previously suggested (Maldonado-Gómez et al., 2016, Tannock et al., 2000). Similarly, we have recently demonstrated that person-specific variations in microbiome composition and function may contribute to the variability in glycemic responses to a variety of foods (Zeevi et al., 2015) and synthetic food supplements (Suez et al., 2014). Understanding the molecular basis by which the individualized gut microbiome resists the colonization of exogenous bacterial strains in some cases, but not in others, may enable counteracting this resistance, thereby leading to reproducible downstream probiotics-mediated effects on currently resistant human hosts. It is important to note that the conclusions reached in our study are based on the use of one multi-strain probiotic preparation by healthy adults. Patterns of colonization resistance upon use of other probiotics strains, or by population subsets not included in our studies, such as children, the elderly and individuals with existing medical conditions merit further prospective human studies. Likewise, our study is not aimed or powered to delineate effects, or lack thereof, of probiotics on mammalian clinical features. It does suggest, at least for the tested probiotics utilized in our studies, that any global host transcriptional effects directly

stemming from mucosal probiotic attachment are individualized at best. As such, mucosa-associated probiotic strains were transiently detected, even in "permissive" individuals, only during consumption or shortly thereafter.

Finally, the identified baseline microbial and host factors potentially enabling prediction of a probiotics-permissive or -resistant state merit validation in larger cohorts and call for consideration of a transition from an empiric "one size fits all" probiotics regimen design, to one which is based on the consumer. Such a measurement-based approach would enable integration of person-specific features in tailoring particular probiotics interventions for a particular person at differing clinical contexts. We thus view our results as an opportunity to harness next-generation sequencing and associated analytics, while taking advantage of inter-individual variability, in devising therapies enabling persistent live-bacteria colonization impacting the host gut mucosa in homeostasis and a variety of microbiome-associated conditions.

STAR★METHODS

Detailed methods are provided in the online version of this paper and include the following:

- KEY RESOURCES TABLES
- CONTACT FOR REAGENT AND RESOURCE SHARING
- EXPERIMENTAL MODEL AND SUBJECT DETAILS
  ○ Clinical trial
  ○ Exclusion and inclusion criteria (human cohorts)
  ○ Human Study Design
- METHOD DETAILS
  ○ Drugs and biological preparations
  ○ Gut microbiome sampling
  ○ Mouse study design
  ○ Bacterial cultures
  ○ Nucleic acid extraction
  ○ Nucleic acid processing and library preparation
- DATA AVAILABILITY

(E and F) MetaPhlAn2-based (E) PCA and (F) Bray-Curtis dissimilarity indices separating permissive and resistant individuals in the LGI after 21 days of probiotics consumption. Significance: Mann-Whitney for (F).

(G) Same as B, but in the LGI mucosa.

(H) Fecal alpha diversity before and during probiotics supplementation in both groups, normalized to baseline. Inset: area under the distance to baseline curve during supplementation, from baseline and excluding days 1-3. Significance: Mann-Whitney.

(I and J) Bacterial load as quantified by qPCR of the 16S rDNA gene and normalized to baseline in (I) stool samples, significance: Kruskal-Wallis & Dunn's, or (J) the LGI mucosa, significance: Mann-Whitney.

(K) Host pathways that significantly distinguish between permissive and resistant individuals in the cecum following probiotics supplementation, FDR corrected. Horizontal lines or symbols represent the mean, error bars SEM or 10–90 percentiles.

See also Figure S8.

AUTHOR CONTRIBUTIONS

N.Z., G.Z.-S, J.S., and U.M. designed, performed and interpreted the experiments, wrote the manuscript, and equally contributed to the study. M.D.-B, S.B., S.F., R.L, H.S., and M.P.-F. performed and assisted in experiments and sample processing. E.K., Y.C, D.R., and I.S. performed computational analyses. A.E.M, S.B.-M., and S.I assisted with RNA sequencing. M.Z., D.R.-L, R.B-Z.B, N.M, and O.S. assisted with patient allocation, follow-up and procedures. A.H. oversaw animal experimentation, including in germ-free mice. Z.H. E.S., and E.E. conceived the study, supervised the participants, interpreted the experiments, and wrote the manuscript.

DECLARATION OF INTERESTS

The authors declare no competing interests. Results of this work have been submitted as a patent proposal.

SUPPORTING CITATIONS

The following references appear in the Supplemental Information: (Furet et al., 2004), (Haarman and Knol, 2005), (Herbel et al., 2013), (Ruggirello et al., 2014), and (Schwendimann, et al., 2015).

REFERENCES

Adiconis, X., Borges-Rivera, D., Satija, R., DeLuca, D.S., Busby, M.A., Berlin, A.M., Sivachenko, A., Thompson, D.A., Wysoker, A., Fennell, T., et al. (2013). Comparative analysis of RNA sequencing methods for degraded or low-input samples. Nat. Methods 10, 623–629.

Bafeta, A., Koh, M., Riveros, C., and Ravaud, P. (2018). Harms Reporting in Randomized Controlled Trials of Interventions Aimed at Modifying Microbiota: A Systematic Review. Ann. Intern. Med. https://doi.org/10.7326/M18-0343.

Bernet, M.-F., Brassart, D., Neeser, J.-R., and Servin, A.L. (1994). Lactobacillus acidophilus LA 1 binds to cultured human intestinal cell lines and inhibits cell attachment and cell invasion by enterovirulent bacteria. Gut 35, 483–489.

Besselink, M.G., van Santvoort, H.C., Buskens, E., Boermeester, M.A., van Goor, H., Timmerman, H.M., Nieuwenhuijs, V.B., Bollen, T.L., van Ramshorst, B., Witteman, B.J., et al.; Dutch Acute Pancreatitis Study Group (2008). Probiotic prophylaxis in predicted severe acute pancreatitis: a randomised, double-blind, placebo-controlled trial. Lancet 371, 651–659.

Bik, E.M., Eckburg, P.B., Gill, S.R., Nelson, K.E., Purdom, E.A., Francois, F., Perez-Perez, G., Blaser, M.J., and Relman, D.A. (2006). Molecular analysis of the bacterial microbiota in the human stomach. Proc. Natl. Acad. Sci. USA 103, 732–737.

Bolger, A.M., Lohse, M., and Usadel, B. (2014). Trimmomatic: a flexible trimmer for Illumina sequence data. Bioinformatics 30, 2114–2120.

Caporaso, J.G., Kuczynski, J., Stombaugh, J., Bittinger, K., Bushman, F.D., Costello, E.K., Fierer, N., Peña, A.G., Goodrich, J.K., Gordon, J.I., et al. (2010). QIIME allows analysis of high-throughput community sequencing data. Nat. Methods 7, 335–336.

Charbonneau, D., Gibb, R.D., and Quigley, E.M. (2013). Fecal excretion of Bifidobacterium infantis 35624 and changes in fecal microbiota after eight weeks of oral supplementation with encapsulated probiotic. Gut Microbes 4, 201–211.

Clarke, T.C., Black, L.I., Stussman, B.J., Barnes, P.M., and Nahin, R.L. (2015). Trends in the use of complementary health approaches among adults: United States, 2002-2012. Natl. Health Stat. Rep. 79, 1–16.

Crovesy, L., Ostrowski, M., Ferreira, D.M.T.P., Rosado, E.L., and Soares-Mota, M. (2017). Effect of Lactobacillus on body weight and body fat in overweight subjects: a systematic review of randomized controlled clinical trials. Int. J. Obes. 41, 1607–1614.

Degnan, F.H. (2012). Clinical studies involving probiotics: when FDA's investigational new drug rubric applies-and when it may not. Gut Microbes 3, 485–489.

Del Piano, M., Carmagnola, S., Andorno, S., Pagliarulo, M., Tari, R., Mogna, L., Strozzi, G.P., Sforza, F., and Capurso, L. (2010). Evaluation of the intestinal colonization by microencapsulated probiotic bacteria in comparison with the same uncoated strains. J. Clin. Gastroenterol. 44 (Suppl 1), S42–S46.

Donaldson, G.P., Lee, S.M., and Mazmanian, S.K. (2016). Gut biogeography of the bacterial microbiota. Nat. Rev. Microbiol. 14, 20–32.

Drago, L., Toscano, M., De Grandi, R., Casini, V., and Pace, F. (2016). Persisting changes of intestinal microbiota after bowel lavage and colonoscopy. Eur. J. Gastroenterol. Hepatol. 28, 532–537.

Draper, K., Ley, C., and Parsonnet, J. (2017). Probiotic guidelines and physician practice: a cross-sectional survey and overview of the literature. Benef. Microbes 8, 507–519.

Eden, E., Navon, R., Steinfeld, I., Lipson, D., and Yakhini, Z. (2009). GOrilla: a tool for discovery and visualization of enriched GO terms in ranked gene lists. BMC Bioinformatics 10, 48.

Eloe-Fadrosh, E.A., Brady, A., Crabtree, J., Drabek, E.F., Ma, B., Mahurkar, A., Ravel, J., Haverkamp, M., Fiorino, A.M., Botelho, C., et al. (2015). Functional dynamics of the gut microbiome in elderly people during probiotic consumption. MBio 6, e00231-15.

Ferrario, C., Taverniti, V., Milani, C., Fiore, W., Laureati, M., De Noni, I., Stuknyte, M., Chouaia, B., Riso, P., and Guglielmetti, S. (2014). Modulation of fecal Clostridiales bacteria and butyrate by probiotic intervention with Lactobacillus paracasei DG varies among healthy adults. J. Nutr. 144, 1787–1796.

Frese, S.A., Hutkins, R.W., and Walter, J. (2012). Comparison of the colonization ability of autochthonous and allochthonous strains of lactobacilli in the human gastrointestinal tract. Adv. Microbiol. 2, 399.

Fukushima, Y., Kawata, Y., Hara, H., Terada, A., and Mitsuoka, T. (1998). Effect of a probiotic formula on intestinal immunoglobulin A production in healthy children. Int. J. Food Microbiol. 42, 39–44.

Fuller, R. (1991). Probiotics in human medicine. Gut 32, 439–442.

Furet, J.-P., Quénée, P., and Tailliez, P. (2004). Molecular quantification of lactic acid bacteria in fermented milk products using real-time quantitative PCR. Int. J. Food Microbiol. 97, 197–207.

Goldin, B.R., Gorbach, S.L., Saxelin, M., Barakat, S., Gualtieri, L., and Salminen, S. (1992). Survival of Lactobacillus species (strain GG) in human gastrointestinal tract. Dig. Dis. Sci. *37*, 121–128.

Goossens, D., Jonkers, D., Russel, M., Stobberingh, E., Van Den Bogaard, A., and StockbrUgger, R. (2003). The effect of Lactobacillus plantarum 299v on the bacterial composition and metabolic activity in faeces of healthy volunteers: a placebo-controlled study on the onset and duration of effects. Aliment. Pharmacol. Ther. *18*, 495–505.

Goossens, D.A., Jonkers, D.M., Russel, M.G., Stobberingh, E.E., and Stockbrügger, R.W. (2006). The effect of a probiotic drink with Lactobacillus plantarum 299v on the bacterial composition in faeces and mucosal biopsies of rectum and ascending colon. Aliment. Pharmacol. Ther. *23*, 255–263.

Guyonnet, D., Schlumberger, A., Mhamdi, L., Jakob, S., and Chassany, O. (2009). Fermented milk containing Bifidobacterium lactis DN-173 010 improves gastrointestinal well-being and digestive symptoms in women reporting minor digestive symptoms: a randomised, double-blind, parallel, controlled study. Br. J. Nutr. *102*, 1654–1662.

Haarman, M., and Knol, J. (2005). Quantitative real-time PCR assays to identify and quantify fecal Bifidobacterium species in infants receiving a prebiotic infant formula. Appl. Environ. Microbiol. *71*, 2318–2324.

Hanifi, A., Culpepper, T., Mai, V., Anand, A., Ford, A.L., Ukhanova, M., Christman, M., Tompkins, T.A., and Dahl, W.J. (2015). Evaluation of Bacillus subtilis R0179 on gastrointestinal viability and general wellness: a randomised, double-blind, placebo-controlled trial in healthy adults. Benef. Microbes *6*, 19–27.

He, F., Ouwehand, A.C., Isolauri, E., Hosoda, M., Benno, Y., and Salminen, S. (2001). Differences in composition and mucosal adhesion of bifidobacteria isolated from healthy adults and healthy seniors. Curr. Microbiol. *43*, 351–354.

Hecht, G., Bar-Nathan, C., Milite, G., Alon, I., Moshe, Y., Greenfeld, L., Dotsenko, N., Suez, J., Levy, M., Thaiss, C.A., et al. (2014). A simple cage-autonomous method for the maintenance of the barrier status of germ-free mice during experimentation. Lab. Anim. *48*, 292–297.

Hegarty, J.W., Guinane, C.M., Ross, R.P., Hill, C., and Cotter, P.D. (2017). Lack of Heterogeneity in Bacteriocin Production Across a Selection of Commercial Probiotic Products. Probiotics Antimicrob. Proteins *9*, 459–465.

Herbel, S.R., Lauzat, B., von Nickisch-Rosenegk, M., Kuhn, M., Murugaiyan, J., Wieler, L.H., and Guenther, S. (2013). Species-specific quantification of probiotic lactobacilli in yoghurt by quantitative real-time PCR. J. Appl. Microbiol. *115*, 1402–1410.

Honeycutt, T.C., El Khashab, M., Wardrop, R.M., 3rd, McNeal-Trice, K., Honeycutt, A.L., Christy, C.G., Mistry, K., Harris, B.D., Meliones, J.N., and Kocis, K.C. (2007). Probiotic administration and the incidence of nosocomial infection in pediatric intensive care: a randomized placebo-controlled trial. Pediatr. Crit. Care Med. *8*, 452–458, quiz 464.

Human Microbiome Project Consortium (2012). Structure, function and diversity of the healthy human microbiome. Nature *486*, 207–214.

Hyatt, D., Chen, G.L., Locascio, P.F., Land, M.L., Larimer, F.W., and Hauser, L.J. (2010). Prodigal: prokaryotic gene recognition and translation initiation site identification. BMC Bioinformatics *11*, 119.

Jacobsen, C.N., Rosenfeldt Nielsen, V., Hayford, A.E., Møller, P.L., Michaelsen, K.F., Paerregaard, A., Sandström, B., Tvede, M., and Jakobsen, M. (1999). Screening of probiotic activities of forty-seven strains of Lactobacillus spp. by in vitro techniques and evaluation of the colonization ability of five selected strains in humans. Appl. Environ. Microbiol. *65*, 4949–4956.

Kanehisa, M., and Goto, S. (2000). KEGG: kyoto encyclopedia of genes and genomes. Nucleic Acids Res. *28*, 27–30.

Kaushik, J.K., Kumar, A., Duary, R.K., Mohanty, A.K., Grover, S., and Batish, V.K. (2009). Functional and probiotic attributes of an indigenous isolate of Lactobacillus plantarum. PLoS ONE *4*, e8099.

Kristensen, N.B., Bryrup, T., Allin, K.H., Nielsen, T., Hansen, T.H., and Pedersen, O. (2016). Alterations in fecal microbiota composition by probiotic supplementation in healthy adults: a systematic review of randomized controlled trials. Genome Med. *8*, 52.

Lahti, L., Salonen, A., Kekkonen, R.A., Salojärvi, J., Jalanka-Tuovinen, J., Palva, A., Orešič, M., and de Vos, W.M. (2013). Associations between the human intestinal microbiota, Lactobacillus rhamnosus GG and serum lipids indicated by integrated analysis of high-throughput profiling data. PeerJ *1*, e32.

Langmead, B., and Salzberg, S.L. (2012). Fast gapped-read alignment with Bowtie 2. Nat. Methods *9*, 357–359.

Laursen, M.F., Laursen, R.P., Larnkjær, A., Michaelsen, K.F., Bahl, M.I., and Licht, T.R. (2017). Administration of two probiotic strains during early childhood does not affect the endogenous gut microbiota composition despite probiotic proliferation. BMC Microbiol. *17*, 175.

Lee, Y.K., Lim, C.Y., Teng, W.L., Ouwehand, A.C., Tuomola, E.M., and Salminen, S. (2000). Quantitative approach in the study of adhesion of lactic acid bacteria to intestinal cells and their competition with enterobacteria. Appl. Environ. Microbiol. *66*, 3692–3697.

Li, X., Brock, G.N., Rouchka, E.C., Cooper, N.G.F., Wu, D., O'Toole, T.E., Gill, R.S., Eteleeb, A.M., O'Brien, L., and Rai, S.N. (2017). A comparison of per sample global scaling and per gene normalization methods for differential expression analysis of RNA-seq data. PLoS ONE *12*, e0176185.

Maldonado-Gómez, M.X., Martínez, I., Bottacini, F., O'Callaghan, A., Ventura, M., van Sinderen, D., Hillmann, B., Vangay, P., Knights, D., Hutkins, R.W., and Walter, J. (2016). Stable Engraftment of Bifidobacterium longum AH1206 in the Human Gut Depends on Individualized Features of the Resident Microbiome. Cell Host Microbe *20*, 515–526.

Manor, O., and Borenstein, E. (2017). Revised computational metagenomic processing uncovers hidden and biologically meaningful functional variation in the human microbiome. Microbiome *5*, 19.

Martin, F.P., Wang, Y., Sprenger, N., Yap, I.K., Lundstedt, T., Lek, P., Rezzi, S., Ramadan, Z., van Bladeren, P., Fay, L.B., et al. (2008). Probiotic modulation of symbiotic gut microbial-host metabolic interactions in a humanized microbiome mouse model. Mol. Syst. Biol. *4*, 157.

McKean, J., Naug, H., Nikbakht, E., Amiet, B., and Colson, N. (2017). Probiotics and Subclinical Psychological Symptoms in Healthy Participants: A Systematic Review and Meta-Analysis. J. Altern. Complement. Med. *23*, 249–258.

McNulty, N.P., Yatsunenko, T., Hsiao, A., Faith, J.J., Muegge, B.D., Goodman, A.L., Henrissat, B., Oozeer, R., Cools-Portier, S., Gobert, G., et al. (2011). The impact of a consortium of fermented milk strains on the gut microbiome of gnotobiotic mice and monozygotic twins. Sci. Transl. Med. *3*, 106ra106.

Mowat, A.M., and Agace, W.W. (2014). Regional specialization within the intestinal immune system. Nat. Rev. Immunol. *14*, 667–685.

O'Brien, C.L., Allison, G.E., Grimpen, F., and Pavli, P. (2013). Impact of colonoscopy bowel preparation on intestinal microbiota. PLoS ONE *8*, e62815.

Ouwehand, A.C., Salminen, S., and Isolauri, E. (2002). Probiotics: an overview of beneficial effects. Antonie van Leeuwenhoek *82*, 279–289.

Panigrahi, P., Parida, S., Nanda, N.C., Satpathy, R., Pradhan, L., Chandel, D.S., Baccaglini, L., Mohapatra, A., Mohapatra, S.S., Misra, P.R., et al. (2017). A randomized synbiotic trial to prevent sepsis among infants in rural India. Nature *548*, 407–412.

Peng, Y., Leung, H.C., Yiu, S.-M., and Chin, F.Y. (2012). IDBA-UD: a de novo assembler for single-cell and metagenomic sequencing data with highly uneven depth. Bioinformatics *28*, 1420–1428.

Qin, J., Li, R., Raes, J., Arumugam, M., Burgdorf, K.S., Manichanh, C., Nielsen, T., Pons, N., Levenez, F., and Yamada, T. (2010). A human gut microbial gene catalogue established by metagenomic sequencing. Nature *464*, 59–65.

Rijkers, G.T., de Vos, W.M., Brummer, R.J., Morelli, L., Corthier, G., and Marteau, P. (2011). Health benefits and health claims of probiotics: bridging science and marketing. Br. J. Nutr. *106*, 1291–1296.

Rochet, V., Rigottier-Gois, L., Sutren, M., Krementscki, M.N., Andrieux, C., Furet, J.P., Tailliez, P., Levenez, F., Mogenet, A., Bresson, J.L., et al. (2006). Effects of orally administered Lactobacillus casei DN-114 001 on the composition or activities of the dominant faecal microbiota in healthy humans. Br. J. Nutr. *95*, 421–429.

Rondanelli, M., Faliva, M.A., Perna, S., Giacosa, A., Peroni, G., and Castellazzi, A.M. (2017). Using probiotics in clinical practice: Where are we now? A review of existing meta-analyses. Gut Microbes 8, 521–543.

Ruggirello, M., Dolci, P., and Cocolin, L. (2014). Detection and viability of Lactococcus lactis throughout cheese ripening. PLoS ONE 9, e114280.

Saldanha, L.G. (2008). US Food and Drug Administration regulations governing label claims for food products, including probiotics. Clin. Infect. Dis. 46, Suppl 2, S119-21; discussion S144-51.

Schwendimann, L., Kauf, P., Fieseler, L., Gantenbein-Demarchi, C., and Miescher Schwenninger, S. (2015). Development of a quantitative PCR assay for rapid detection of Lactobacillus plantarum and Lactobacillus fermentum in cocoa bean fermentation. J. Microbiol. Methods 115, 94–99.

Senok, A.C., Ismaeel, A.Y., and Botta, G.A. (2005). Probiotics: facts and myths. Clin. Microbiol. Infect. 11, 958–966.

Sharon, I., Morowitz, M.J., Thomas, B.C., Costello, E.K., Relman, D.A., and Banfield, J.F. (2013). Time series community genomics analysis reveals rapid shifts in bacterial species, strains, and phage during infant gut colonization. Genome Res. 23, 111–120.

Sharon, I., Kertesz, M., Hug, L.A., Pushkarev, D., Blauwkamp, T.A., Castelle, C.J., Amirebrahimi, M., Thomas, B.C., Burstein, D., Tringe, S.G., et al. (2015). Accurate, multi-kb reads resolve complex populations and detect rare microorganisms. Genome Res. 25, 534–543.

Sierra, S., Lara-Villoslada, F., Sempere, L., Olivares, M., Boza, J., and Xaus, J. (2010). Intestinal and immunological effects of daily oral administration of Lactobacillus salivarius CECT5713 to healthy adults. Anaerobe 16, 195–200.

Suez, J., Korem, T., Zeevi, D., Zilberman-Schapira, G., Thaiss, C.A., Maza, O., Israeli, D., Zmora, N., Gilad, S., Weinberger, A., et al. (2014). Artificial sweeteners induce glucose intolerance by altering the gut microbiota. Nature 514, 181–186.

Suez, J., Zmora, N., Zilberman-Schapira, G., Mor, U., Dori-Bachash, M., Bashiardes, S., Zur, M., Regev-Lehavi, D., Brik, R.B.-Z., Federici, S., et al. (2018). Post-Antibiotic Gut Mucosal Microbiome Reconstitution Is Impaired by Probiotics and Improved by Autologous FMT. Cell 174, this issue, 1406–1423.

Sun, J., and Buys, N.J. (2016). Glucose- and glycaemic factor-lowering effects of probiotics on diabetes: a meta-analysis of randomised placebo-controlled trials. Br. J. Nutr. 115, 1167–1177.

Tannock, G.W., Munro, K., Harmsen, H.J., Welling, G.W., Smart, J., and Gopal, P.K. (2000). Analysis of the fecal microflora of human subjects consuming a probiotic product containing Lactobacillus rhamnosus DR20. Appl. Environ. Microbiol. 66, 2578–2588.

Truong, D.T., Franzosa, E.A., Tickle, T.L., Scholz, M., Weingart, G., Pasolli, E., Tett, A., Huttenhower, C., and Segata, N. (2015). MetaPhlAn2 for enhanced metagenomic taxonomic profiling. Nat. Methods 12, 902–903.

Tuomola, E., Crittenden, R., Playne, M., Isolauri, E., and Salminen, S. (2001). Quality assurance criteria for probiotic bacteria. Am. J. Clin. Nutr. 73 (2, Suppl), 393S–398S.

Turroni, F., Serafini, F., Foroni, E., Duranti, S., O'Connell Motherway, M., Taverniti, V., Mangifesta, M., Milani, C., Viappiani, A., Roversi, T., et al. (2013). Role of sortase-dependent pili of Bifidobacterium bifidum PRL2010 in modulating bacterium-host interactions. Proc. Natl. Acad. Sci. USA 110, 11151–11156.

Van Tassell, M.L., and Miller, M.J. (2011). Lactobacillus adhesion to mucus. Nutrients 3, 613–636.

Vogel, G. (2008). Clinical Trials. Deaths prompt a review of experimental probiotic therapy. Science 319, 557.

Wang, C., Nagata, S., Asahara, T., Yuki, N., Matsuda, K., Tsuji, H., Takahashi, T., Nomoto, K., and Yamashiro, Y. (2015). Intestinal Microbiota Profiles of Healthy Pre-School and School-Age Children and Effects of Probiotic Supplementation. Ann. Nutr. Metab. 67, 257–266.

Yang, H., Huang, X., Fang, S., Xin, W., Huang, L., and Chen, C. (2016). Uncovering the composition of microbial community structure and metagenomics among three gut locations in pigs with distinct fatness. Sci. Rep. 6, 27427.

Yuan, F., Ni, H., Asche, C.V., Kim, M., Walayat, S., and Ren, J. (2017). Efficacy of Bifidobacterium infantis 35624 in patients with irritable bowel syndrome: a meta-analysis. Curr. Med. Res. Opin. 33, 1191–1197.

Zeevi, D., Korem, T., Zmora, N., Israeli, D., Rothschild, D., Weinberger, A., Ben-Yacov, O., Lador, D., Avnit-Sagi, T., Lotan-Pompan, M., et al. (2015). Personalized Nutrition by Prediction of Glycemic Responses. Cell 163, 1079–1094.

Zhang, Q., Wu, Y., and Fei, X. (2015). Effect of probiotics on body weight and body-mass index: a systematic review and meta-analysis of randomized, controlled trials. Int. J. Food Sci. Nutr. 67, 571–580.

Zmora, N., Zeevi, D., Korem, T., Segal, E., and Elinav, E. (2016). Taking it Personally: Personalized Utilization of the Human Microbiome in Health and Disease. Cell Host Microbe 19, 12–20.

STAR★METHODS

KEY RESOURCES TABLES

REAGENT or RESOURCE	SOURCE	IDENTIFIER
Bacterial and Virus Strains		
Lactobacillus acidophilus	N/A	Cat# ATCC 4356
Lactobacillus rhamnosus	Clinical isolate	N/A
Lactobacillus casei	N/A	Cat# ATCC 393
Lactobacillus casei subsp. *paracasei*	N/A	Cat# ATCC BAA-52
Lactobacillus plantarum	N/A	Cat# ATCC 8014
Bifidobacterium longum subsp. *infantis*	N/A	Cat# ATCC 15697
Bifidobacterium bifidum	N/A	Cat# ATCC 29521
Bifidobacterium breve	N/A	Cat# ATCC 15700
Bifidobacterium longum subsp. *longum*	N/A	Cat# ATCC 15707
Lactococcus lactis	Isolated from Bio 25 Supherb	N/A
Streotococcus thermophilus	N/A	Cat# ATCC BAA-491
Chemicals, Peptides, and Recombinant Proteins		
Bio 25 Supherb	Supherb Ltd, Nazareth Ilit, Israel	N/A
Critical Commercial Assays		
NextSeq 500/550 High Output v2 kit (150 cycles), for Metagenome shotgun sequencing	illumina	Cat# FC-404-2002
NextSeq 500/550 High Output v2 kit (75 cycles), for RNA-Seq	illumina	Cat# FC-404-2005
MiSeq Reagent Kit v2 (500-cycles)	illumina	Cat# MS-102-2003
RNeasy mini kit	QIAGEN	Cat# 74104
DNeasy PowerLyzer PowerSoil Kit	QIAGEN	Cat# 12855-100
NEBNext Ultra Directional RNA Library Prep Kit for Illumina	New England Biolabs	Cat# E7420S
NEBNext Multiplex Oligos for Illumina	New England Biolabs	Cat# E7600S
Experimental Models: Organisms/Strains		
C57BL/6JOlaHsd males 8-9 weeks of age	Envigo, Israel	N/A
Germ-free Swiss-Webster males 8-9 weeks of age	Weizmann institute of Science	N/A
Deposited Data		
Sequence data	European Nucleotide Archive	ENA: PRJEB28097
Oligonucleotides		
Miseq Illumina sequencing primer Read 1 - TATGGTAATTG TGTGCCAGCMGCCGCGGTAA	N/A	N/A
Miseq Illumina sequencing primer Read 2 - AGTCAGTCAG CCGGACTACHVGGGTWTCTAAT	N/A	N/A
Miseq Illumina sequencing primer Index primer - ATTAGA WACCCBDGTAGTCCGGCTGACTGACT	N/A	N/A
Software and Algorithms		
QIIME	N/A	(Caporaso et al., 2010)
Trimmomatic	N/A	(Bolger et al., 2014)
MetaPhlAn2	N/A	(Truong et al., 2015)
Bowtie2	N/A	(Langmead and Salzberg, 2012)
EMPANADA	N/A	(Manor and Borenstein, 2017)
RNASeq analysis software	GOrilla (Gene Ontology enRIchment anaLysis and visuaLizAtion tool) http://cbl-gorilla.cs.technion.ac.il/	(Eden et al., 2009)

CONTACT FOR REAGENT AND RESOURCE SHARING

Further information and requests for reagents may be directed to and will be fulfilled by Eran Elinav (eran.elinav@weizmann.ac.il).

EXPERIMENTAL MODEL AND SUBJECT DETAILS

Clinical trial

The human MUSPIC trials were approved by the Tel Aviv Sourasky Medical Center Institutional Review Board (IRB approval numbers TLV-0553-12, TLV-0658-12 and TLV-0196-13) and Weizmann Institute of Science Bioethics and Embryonic Stem Cell Research oversight committee (IRB approval numbers 421-1, 430-1 and 444-1), and were reported to http://clinicaltrials.gov/ (Identifiers: NCT03218579 and NCT01922830). Written informed consent was obtained from all subjects.

Exclusion and inclusion criteria (human cohorts)

All subjects fulfilled the following inclusion criteria: males and females, aged 18-70, who are currently not following any diet regimen or dietitian consultation and are able to provide informed consent. Exclusion criteria included: (i) pregnancy or fertility treatments; (ii) usage of antibiotics or antifungals within 3 months prior to participation; (iii) consumption of probiotics in any form within 1 month prior to participation, (iv) chronically active inflammatory or neoplastic disease in the three years prior to enrollment; (v) chronic gastrointestinal disorder, including inflammatory bowel disease and celiac disease; (vi) active neuropsychiatric disorder; (vii) myocardial infarction or cerebrovascular accident in the 6 months prior to participation; (viii) coagulation disorders; (ix) chronic immunosuppressive medication usage; (x) pre-diagnosed type I or type II diabetes mellitus or treatment with anti-diabetic medication. Adherence to inclusion and exclusion criteria was validated by medical doctors.

Human Study Design

Twenty-nine healthy volunteers were recruited for this study between the years 2014 and 2018 (see Table S1). Upon enrollment, participants were required to fill up medical, lifestyle and food frequency questionnaires, which were reviewed by medical doctors before the acceptance to participate in the study. Two cohorts were recruited, a naive cohort (n = 10) and an interventional, placebo-controlled cohort (n = 19), subdivided into 2 interventions of probiotics (n = 14) and placebo pills (n = 5). For the latter cohort, the study design consisted of three phases, baseline (7 days), intervention (28 days) and follow-up (28 days). During the 4-week intervention phase (days 1 through 28), participants from the probiotics arm were instructed to consume a commercial probiotic supplement (Bio-25) bi-daily; participants from the placebo arm were instructed to consume a similar-looking pill bi-daily (see "Drugs and biological preparations"). No dietary variations were noted between the interventional and placebo groups (Fisher's exact p = 0.58). In the intervention/placebo cohort stool samples were collected daily during the baseline phase and during the first week of intervention, and then weekly throughout the rest of the intervention and follow-up phases. Ten participants in the probiotics arm and the entire placebo arm underwent two endoscopic examinations, one immediately before the intervention, at the end of the baseline phase (day 0), and another 3 weeks through the intervention phase (day 21). Participants in the naive cohort underwent a single endoscopic examination; and four participants in the probiotics arm ("validation arm") underwent only a single colonoscopy, 3 weeks into the intervention phase (day 21). The trial was completed as planned in 28 subjects. In this trial, 7 minor adverse events were reported and all fully resolved. One participant developed a serious adverse event after the first colonoscopy, was treated to full recovery and excluded from the rest of the study. All participants received payment for their participation in the study upon discharge from their last endoscopic session. Throughout the entire study 248 luminal, 483 mucosal, 320 stool samples, and 242 regional biopsies, were collected.

METHOD DETAILS

Drugs and biological preparations
Probiotics

During the probiotics phase participants consumed Superherb Bio-25 bi-daily, which is described by the manufacturer to contain at least 25 billion active bacteria of the following strains: *B. bifidum, L. rhamnosus, L. lactis, L. casei, B. breve, S. thermophilus, B. longum* sbsp. *longum, L. paracasei, L. plantarum* and *B. longum* sbsp. *infantis.* According to the manufacturer, the pills underwent double coating to ensure their survival under stomach acidity and their proliferation in the intestines. Validation of the aforementioned strains quantity and viability was performed as part of the study, see **figure S4A-E**. Probiotics colonization in humans was cross-validated by four different methods, including genus-level determination by 16S rDNA analysis; phylogenetic analysis of shotgun metagenomic sequences based on bacterial marker genes (MetaPhlAn2); amplification of the probiotics targets with qPCR; and strain-level analysis on shotgun metagenomic sequences based on unique genomic sequences (Sharon et al., 2015).

Placebo pills

Placebo pills (Trialog, Inc.) were composed of a hydroxypropylmethyl cellulose (HPMC) capsule, filled with 600 mg microcrystalline cellulose PH.EU (MCC). Placebo pill manufacturing process was approved for pharmaceutical use by the Israeli Ministry of Health, and underwent a microbial burden examination prior to administration. Placebo and probiotic pills were labeled identically to maintain blinding.

Gut microbiome sampling

Stool sampling

Participants were requested to self-sample their stool on pre-determined intervals (as previously described) using a swab following detailed printed instructions. Collected samples were immediately stored in a home freezer ($-20°C$) for no more than 7 days and transferred in a provided cooler to our facilities, where they were stored at $-80°C$.

Endoscopic examination

Forty-eight hours prior to the endoscopic examination, participants were asked to follow a pre-endoscopy diet. 20 hours prior to the examination diet was restricted to clear liquids. All participants underwent a sodium picosulfate (Pico Salax)-based bowel preparation. Participants were equipped with two fleet enemas, which they were advised to use in case of unclear stools. The examination was performed using a Pentax 90i endoscope (Pentax Medical) under light sedation with propofol-midazolam. The effect of bowel preparation on the microbiome was studied in two healthy female participants from the naive cohort (aged 25 and 27, BMI 20.3 and 22.8, respectively, Table S1), who underwent two consecutive colonoscopies. The first was performed in the absence of any form of bowel preparation, followed by a second procedure 3 weeks later performed using a routine Picolax bowel preparation protocol. Luminal content was aspirated from the stomach, duodenum, jejunum, terminal ileum, cecum and descending colon into 15 ml tubes by the endoscope suction apparatus and placed immediately in liquid nitrogen. Brush cytology (US Endoscopy) was used to scrape the gut lining to obtain mucosal content from the gastric fundus, gastric antrum, duodenal bulb, jejunum, terminal ileum, cecum, ascending colon, transverse colon, descending colon, sigmoid colon and rectum. Brushes were placed in screw cap micro tubes and were snap-frozen in liquid nitrogen. Biopsies from the gut epithelium were obtained from the stomach, duodenum, jejunum, terminal ileum, cecum, and descending colon and were snap-frozen in liquid nitrogen. By the end of each session, all samples were transferred to Weizmann Institute of Science and stored in $-80°C$. All the endoscopic procedures were performed using an identical protocol by one of three highly experienced board-certified gastroenterologists in a single tertiary medical center.

Mouse study design

Eight-week old male C57BL/6 mice (average initial weight 20 gr) were purchased from Harlan Envigo and allowed to acclimatize to the animal facility environment for 2 weeks prior to experimentation. Germ-free Swiss-Webster mice were born in the Weizmann Institute germ-free facility, kept in gnotobiotic isolators and routinely monitored for sterility. In all experiments, age- and gender-matched mice were used. All mice were kept at a strict 24 hr light-dark cycle, with lights on from 6am to 6pm. Each experimental group consisted of two cages to control for cage effect. For probiotics supplementation, a single pill (Supherb Bio-25) was dissolved in 10 ml of sterile PBS and immediately fed to mice by oral gavage during the dark phase (4×10^9 CFU kg^{-1} day^{-1}). For conventionalization of GF mice, 200 mg of frozen human stool samples were resuspended in sterile PBS under anaerobic conditions (Coy Laboratory Products, 75% N_2, 20% CO_2, 5% H_2), vortexed for 3 minutes and allowed to settle by gravity for 2 min. Samples (supernatants) were immediately transferred to the animal facility in Hungate anaerobic culture tubes and the supernatant was administered to germ-free mice by oral gavage. Mice were allowed to conventionalize for three days prior to probiotics treatment, as previously described. Stool was collected on pre-determined days at the beginning of the dark phase, and immediately snap-frozen and transferred for storage at $-80°C$ until further processing. Upon the termination of experiments, mice were sacrificed by CO_2 asphyxiation, and laparotomy was performed by employing a vertical midline incision. After the exposure and removal of the digestive tract, it was dissected into eight parts: the stomach; beginning at the pylorus, the proximal 4 cm of the small intestine was collected as the duodenum; the following third of the small intestine was collected as the proximal and distal jejunum; the ileum was harvested as the distal third of the small intestine; the cecum; lastly, the colon was divided into its proximal and distal parts. For each section, the content within the cavity was extracted and collected for luminal microbiome isolation, and the remaining tissue was rinsed three times with sterile PBS and collected for mucosal microbiome isolation. During each time point, each group was handled by a different researcher in one biological hood to minimize cross-contamination. All animal studies were approved by the Weizmann Institute of Science Institutional Animal Care and Use committee (IACUC), application number 29530816-2.

Bacterial cultures

Bacterial strains used in this study are listed in Key Resource Table. *Lactobacillus* strains were grown in De Man, Rogosa and Sharpe (MRS) broth or agar, *Bifidobacterium* strains in modified Bifidobacterium agar or modified reinforced clostridial broth, *Lactococcus* and *Streptococcus* were grown in liquid or solid M17 medium. Liquid or solid Brain-Heart Infusion (BHI) was used for non-selective growth of probiotic bacteria. Cultures were grown under anaerobic conditions (Coy Laboratory Products, 75% N_2, 20% CO_2, 5% H_2) in $37°C$ without shaking. All growth media were purchased from BD. For enumeration of viable bacteria from the probiotics pill, a single pill (Supherb Bio-25) was dissolved in 10 ml of sterile PBS and serially diluted and plated on all growth media.

Nucleic acid extraction
DNA purification

DNA was isolated from endoscopic samples, both luminal content and mucosal brushes, using DNeasy PowerLyzer PowerSoil Kit (QIAGEN). DNA was isolated from stool swabs using PowerMag Soil DNA Isolation Kit (QIAGEN) optimized for an automated platform.

RNA Purification

Gastrointestinal biopsies obtained from the participants were purified using RNAeasy kit (QIAGEN, 74104) according to the manufacturer's instructions. Most of the biopsies were kept in RNAlater solution (ThermoFisher, AM7020) and were immediately frozen in liquid nitrogen.

Nucleic acid processing and library preparation
qPCR Protocol for Quantification of Bacterial DNA

DNA templates were diluted to a final amount of 1 ng per reaction. Amplifications were performed with the primer sets (indicated in Table S4) using the Fast SYBR^{TM} Green Master Mix (ThermoFisher) in duplicates. Amplification conditions were: denaturation 95°C for 3 minutes, followed by 40 cycles of denaturation 95°C for 3 s; annealing 64°C for 30 s followed by melting curve. Duplicates with >2 cycle difference were excluded from analysis. The CT value for any sample not amplified after 40 cycles was defined as 40 (threshold of detection).

16S rDNA Sequencing

For 16S amplicon pyrosequencing, PCR amplification was performed spanning the V4 region using the primers 515F/806R of the 16S rRNA gene and subsequently sequenced using 2 × 250 bp paired-end sequencing (Illumina MiSeq). Custom primers were added to Illumina MiSeq kit resulting in 253 bp fragment sequenced following paired end joining to a depth of 110,998 ± 66,946 reads (mean ± SD).

Read1: TATGGTAATTGTGTGCCAGCMGCCGCGGTAA
Read2: AGTCAGTCAGCCGGACTACHVGGGTWTCTAAT
Index sequence primer: ATTAGAWACCCBDGTAGTCCGGCTGACTGACTATTAGAA

Whole genome shotgun sequencing

100 ng of purified DNA was sheared with a Covaris E220X sonicator. Illumina compatible libraries were prepared as described (Suez et al., 2014), and sequenced on the Illumina NextSeq platform with a read length of 80 bp to a depth of 5,041,171 ± 3,707,376 (mean ± SD) reads for stool samples and 2,000,661 ± 4,196,093 (mean ± SD) for endoscopic samples.

RNA-Seq

Ribosomal RNA was selectively depleted by RnaseH (New England Biolabs, M0297) according to a modified version of a published method (Adiconis et al., 2013). Specifically, a pool of 50 bp DNA oligos (25 nM, IDT, indicated in Table S5) that is complementary to murine rRNA 18S and 28S, was resuspended in 75 μl of 10 mM Tris pH 8.0. Total RNA (100-1000 ng in 10 μl H_2O) were mixed with an equal amount of rRNA oligo pool, diluted to 2 μl and 3 μl 5x rRNA hybridization buffer (0.5 M Tris-HCl, 1 M NaCl, titrated with HCl to pH 7.4) was added. Samples were incubated at 95°C for 2 minutes, then the temperature was slowly decreased (−0.1°C/s) to 37°C. RNaseH enzyme mix (2 μl of 10 U RNaseH, 2 μl 10x RNaseH buffer, 1 μl H_2O, total 5 μl mix) was prepared 5 minutes before the end of the hybridization and preheated to 37°C. The enzyme mix was added to the samples when they reached 37°C and they were incubated at this temperature for 30 minutes. Samples were purified with 2.2x SPRI beads (Ampure XP, Beckmann Coulter) according to the manufacturers' instructions. Residual oligos were removed with DNase treatment (ThermoFisher Scientific, AM2238) by incubation with 5μl DNase reaction mix (1 μl Trubo DNase, 2.5 μl Turbo DNase 10x buffer, 1.5 μl H_2O) that was incubated at 37°C for 30 minutes. Samples were again purified with 2.2x SPRI beads and suspended in 3.6 μl priming mix (0.3 μl random primers of New England Biolab, E7420, 3.3 μl H_2O). Samples were subsequently primed at 65°C for 5 minutes. Samples were then transferred to ice and 2 μl of the first strand mix was added (1 μl 5x first strand buffer, NEB E7420; 0.125 μl RNase inhibitor, NEB E7420; 0.25 μl ProtoScript II reverse transcriptase, NEB E7420; and 0.625 μl of 0.2 μg/μl Actinomycin D, Sigma, A1410). The first strand synthesis and all subsequent library preparation steps were performed using NEBNext Ultra Directional RNA Library Prep Kit for Illumina (NEB, E7420) according to the manufacturers' instructions (all reaction volumes reduced to a quarter).

16S rDNA analysis

The 2 × 250 bp reads were processed using the QIIME (Caporaso et al., 2010) (Quantitative Insights Into Microbial Ecology, http://www.qiime. org) analysis pipeline. In brief, FASTA quality files and a mapping file indicating the barcode sequence corresponding to each sample were used as inputs. Paired reads were first assembled into longer reads based on sequence similarity, and then split to samples according to the barcodes. Sequences sharing >97% nucleotide sequence identity in the 16S rRNA region were binned into operational taxonomic units (97% ID OTUs). Each OTU was assigned a taxonomical classification by applying the Uclust algorithm against the Greengenes database, and an OTU table was created.

Metagenomic analysis

Data from the sequencer was converted to fastq files with bcl2fastq. Reads were then QC trimmed using Trimmomatic (Bolger et al., 2014) with parameters PE -threads 10 -phred33 -validatePairs ILLUMINACLIP:TruSeq3-PE.fa:2:30:10 LEADING:3 TRAILING:3 MINLEN:50. We used MetaPhlAn2 (Truong et al., 2015) for taxonomic analysis with the parameters: –ignore_viruses –ignore_archaea –ignore _eukaryotes.

Host sequences were removed by aligning the reads against human genome reference hg19 using bowtie2 (Langmead and Salzberg, 2012) with the parameters: -D 5 -R 1 -N 0 -L 22 -i S,0,2.50. The resulting non-host reads were then mapped to the integrated gene catalog (Qin et al., 2010) using bowtie2 with parameters:–local -D 25 -R 3 -N 1 -L 19 -i S,1,0.25 -k 5 allowing to a single read to match up to five different entries.

Further filtering of the bacterial reads consisted of retaining only records with minimal base quality of 26. The resulting bacterial quality-filtered bam files were then subsampled to 1×10^5 and 5×10^5 bacterial hits for endoscopic and stool samples, respectively. An entry's score was defined by its length, divided by the gene length. Entries' scores were summarized according to KO annotations (Kanehisa and Goto, 2000). Each sample was scaled to 1M. KEGG Pathway analysis was conducted using EMPANADA (Manor and Borenstein, 2017).

Probiotics strain identification by unique genomic sequences

To evaluate the presence of the probiotic strains using metagenomics data we applied a pipeline aimed at determining whether a strain's species is present in the sample, and then whether one of the strains for the species in the sample is the probiotics strain.

Preparation step: genome recovery of probiotics strains - Genomes of the probiotic strains were reconstructed from metagenomics samples of the probiotics pills used in the study. Assembly was performed using idba-ud (Peng et al., 2012), followed by genome closing procedures that relied on connecting scaffolds using paired-end read data and mini-assembly (Sharon et al., 2013). Genomes for the most abundant strains were recovered first using part of the data. Less abundant genomes were recovered next after removing the reads for the abundant genomes from the samples and using all the remaining data. Genes and proteins were predicted for each genome using prodigal (Hyatt et al., 2010). The abundance of different strains was evaluated and the amount of data required for each genome was estimated by MetaPhlAn2 (Truong et al., 2015). Statistics for the recovered genomes and closest published strains are provided in Table S6. All genomes but *B. longum* were assembled at an estimated completeness of >94% and contamination of <4%. *B. longum* was probably represented by two strains, of which we were able to assemble and identify the common regions (roughly half of the genome sizes). All probiotic strains but *L. lactis* and *L. paracasei* had nearly identical published reference genomes.

Evaluating the presence of probiotics strains in metagenomics samples

1. **Removal of human reads from samples.** Metagenomic reads were mapped against the human genome (GRCh38.p7, downloaded from NCBI) using bowtie2 (Langmead and Salzberg, 2012) with the parameter:–very_sensitive. All read pairs, in which one or both reads aligned to the genome, were removed from further analysis.
2. **Identifying reads that potentially belong to the probiotic strains.** Metagenomic reads were mapped against the recovered probiotic genomes using bowtie2 with the parameter:–very_sensitive. All mapped reads and their paired-ends were considered further in the analysis.
3. **Assigning reads to probiotic genomes.** All reads recovered in the previous step were aligned against a database consisting of all probiotic genomes as well as genomes downloaded from RefSeq, which belong to the orders Bifidobacteriales and Lactobacillales (maximum of 10 genomes for each species). Alignment was done using bowtie2 with the parameter:–very_sensitive. Reads that best aligned to one of the probiotic strains were assigned to the strain along with their paired-end.
4. **Determining species presence in each sample.** For each probiotic strain, the percent of its genes expected to be covered by at least one read was estimated as a function of the observed genome coverage. This was done through simulations, in which different numbers of reads from one of the metagenomic samples of the probiotic pill were aligned against each of the probiotic genomes. Based on these simulations we designed a function that bound 95% of the simulated samples using R functions loess.sd (package msir) and approxfun. The threshold was set to half of the resulting function value for each coverage.
5. **Identifying strain-specific genes in each probiotic genome.** This step was necessary for the identification of the probiotic strains in the samples (see next step) and included: downloading available genomes of other strains for the same species from NCBI's RefSeq and comparing each reference genome to the probiotic strain genome using compare-sets.pl (https://github.com/CK7/compare-sets) with a 96% similarity threshold. Genomes that aligned at $\geq$ 70% of their length were labeled "similar" while genomes that aligned at $\geq$ 98% of their size were labeled "nearly identical." Then genes of the probiotic strain were aligned against all similar/nearly identical genomes using blastn. A gene was identified as strain-specific gene if it aligned to at least one other genome at > = 60% identity, and aligned to no more than 10% of the similar (but not nearly identical) genomes. Table S7 summarizes the number of genes and strain-specific genes for each probiotic strain.
6. **Determining probiotic strain presence in each sample.** We characterized the presence of strain genes that were expected to be covered by at least one read for each percent of all genes covered by one or more reads using simulations. Based on the simulations we designed functions that bound 95% and 99% of the simulated results using R functions loess.sd and approxfun. Assignment of probiotic strains to species was done according to the following key: "**Unknown**", < 20% of all genes were covered by at least one read; "**Do not contain the probiotic strain**", the fraction of strain specific genes were below the 99% function; "**Possibly contain the probiotic strain**", samples in which the fraction of strain genes was between the 95% to the 99% functions; "**Contain the probiotic strain**", the fraction of strain genes was above the 95% function.

RNA-seq analysis

Data normalization: Initially, we normalized the sequenced data as previously described (Li et al., 2017). Briefly, genes with mean TPM < 1 across all samples were filtered out from the analysis, and a value of 0.001 was added to remaining TPM values to avoid

zero-values in downstream calculations. Then, sample median normalization was performed based on all constitutive gene reads with positive counts for all samples. Thus, all TPM values in each sample were scaled by the median TPM of constitutive reads in that sample, divided by the median TPM across all samples. We then performed a per-gene normalization by dividing each expression value by the median value of that gene across all samples. Finally, expression data was log-transformed (base 2). The above normalization steps were performed separately to data acquired from each of the different experimental batches, determined by the presence or absence of RNAlater solution for sample preservation.

Comparison of expression levels before and after treatment with probiotics: To account for inter-personal differences and reduce noise, we compared the effects of probiotics treatment on host expression patterns using a repeated-measures design. Thus, for each individual, in each biopsy region, the relative fold changes (log, base 2) in expression levels of each gene were calculated between samples taken at baseline and after treatment with probiotics. Then, for each individual, genes were ranked from low to high, and sorted by their median rank across all available samples. These sorted lists were subsequently used for gene ontology (GO) enrichment analysis using Gorilla (Eden et al., 2009) (http://cbl-gorilla.cs.technion.ac.il/) with a p value threshold of 10^{-3} and a false-discovery rate (FDR) threshold of q < 0.05.

Comparison of expression levels between probiotics-persistent and resistant individuals: For each gene, median relative expression was calculated in probiotics-persistent and resistant individuals within each biopsy region and experimental batch. Then, genes were sorted by the ratio (log, base 2) between median relative expression levels across probiotics-persistent compared to resistant individuals. Finally, to combine findings from both experimental batches, we intersected the top and the bottom 10% of the genes across the two batches. Intersected lists were used as target sets for GOrilla GO enrichment analysis as described above, with the entire set of genes that passed the initial filtering as a background set.

Quantification and statistical analysis

The following statistical analyses were applied unless specifically stated otherwise: For 16S data, rare OTUs (< 0.1% in relative abundance) were filtered out, and samples were then rarefied to a depth of 10,000 reads, unless specified otherwise. For metagenomic data, stool samples with $< 5 \times 10^5$ and endoscopic samples with $< 10^5$ assigned bacterial reads (after host removal) were excluded from further analysis. In the remaining samples, rare KEGG orthologous (KO) genes (< 0.1%) were removed. Beta diversity was calculated on OTUs (16S) or species (metagenomics) relative abundances using UniFrac distances or Bray-Curtis dissimilarity (R Vegan package, https://CRAN.R-project.org/package=vegan), respectively. Beta diversity for KOs and functional bacterial pathways was calculated using Spearman's rank correlation coefficient. Alpha diversity was calculated on OTUs (16S) using the observed species index. For 16S data, measurements of alpha and beta diversity were calculated using QIIME tools v 1.9.1. In order to determine the effect of treatment on microbiota taxonomic composition and functional capacity repeated-measures Kruskal Wallis with Dunn's test was used. In order to compare the effect of treatment over time between two groups or more Two-Way ANOVA with Dunnett test, or permutation tests performed by switching labels between participants (in a paired fashion when suitable), including all their assigned samples, were used. Mann-Whitney and Wilcoxon tests were used to conduct pairwise comparisons between two treatment arms or two groups of participants. Permutational multivariate ANOVA (Adonis PERMANOVA with 10,000 permutations) based on sample distances was used to test for changes in the community composition and function. To analyze qPCR data, Two-way ANOVA with Sidak or Dunnett test was used. The threshold of significance was determined to be 0.05 both for p and q-values. Statistically significant findings were marked according to the following cutoffs: *, p < 0.05; **, p < 0.01; ***, p < 0.001; ****, p < 0.0001. Data were plotted with GraphPad Prism version 7.0c. Statistical details for all experiments, including sample size, the statistical test used, dispersion and precision measures and statistical significance, are specified in the result section and denoted in figure legends.

DATA AVAILABILITY

Sequence data have been deposited in the European Nucleotide Archive under accession number ENA: PRJEB28097.
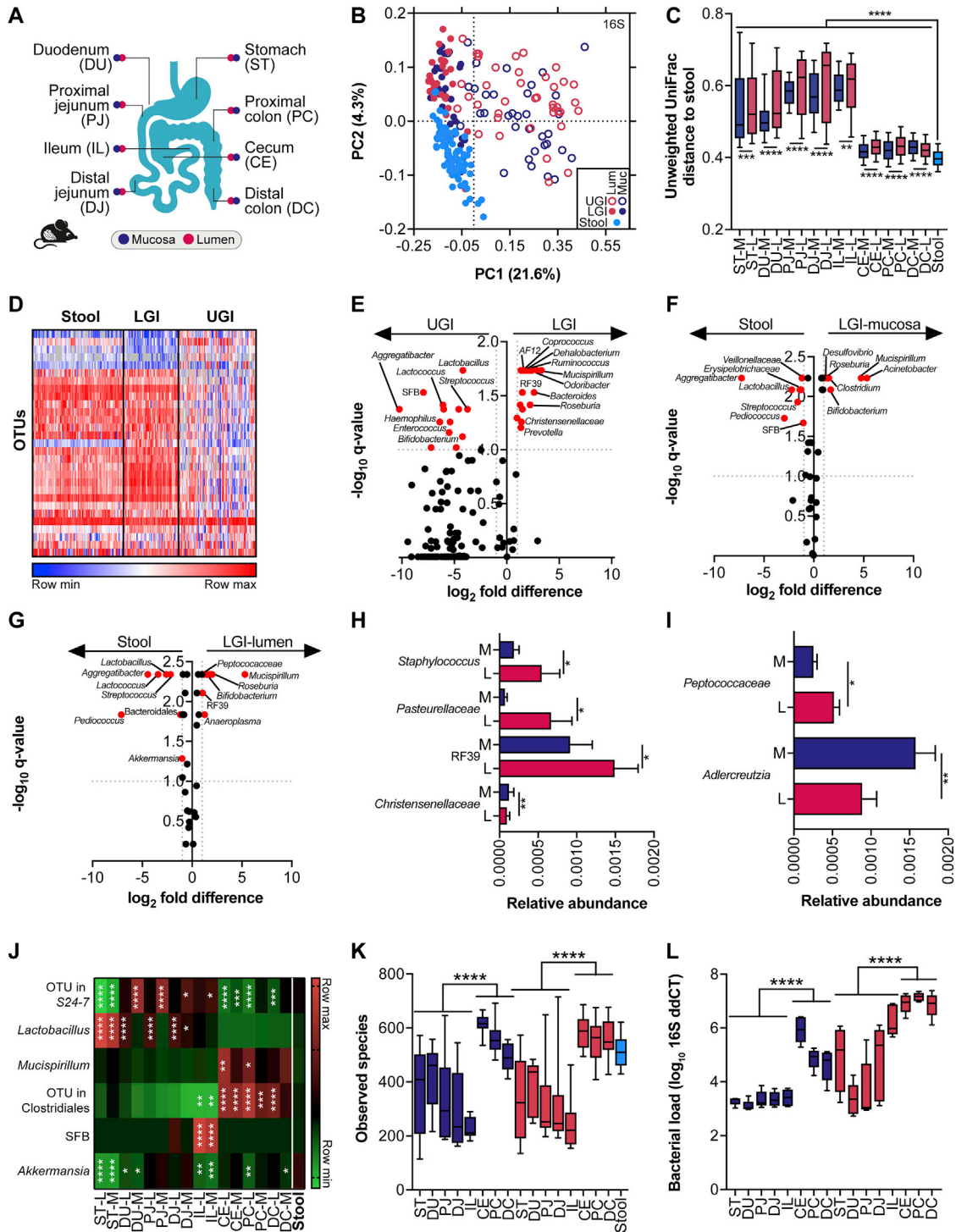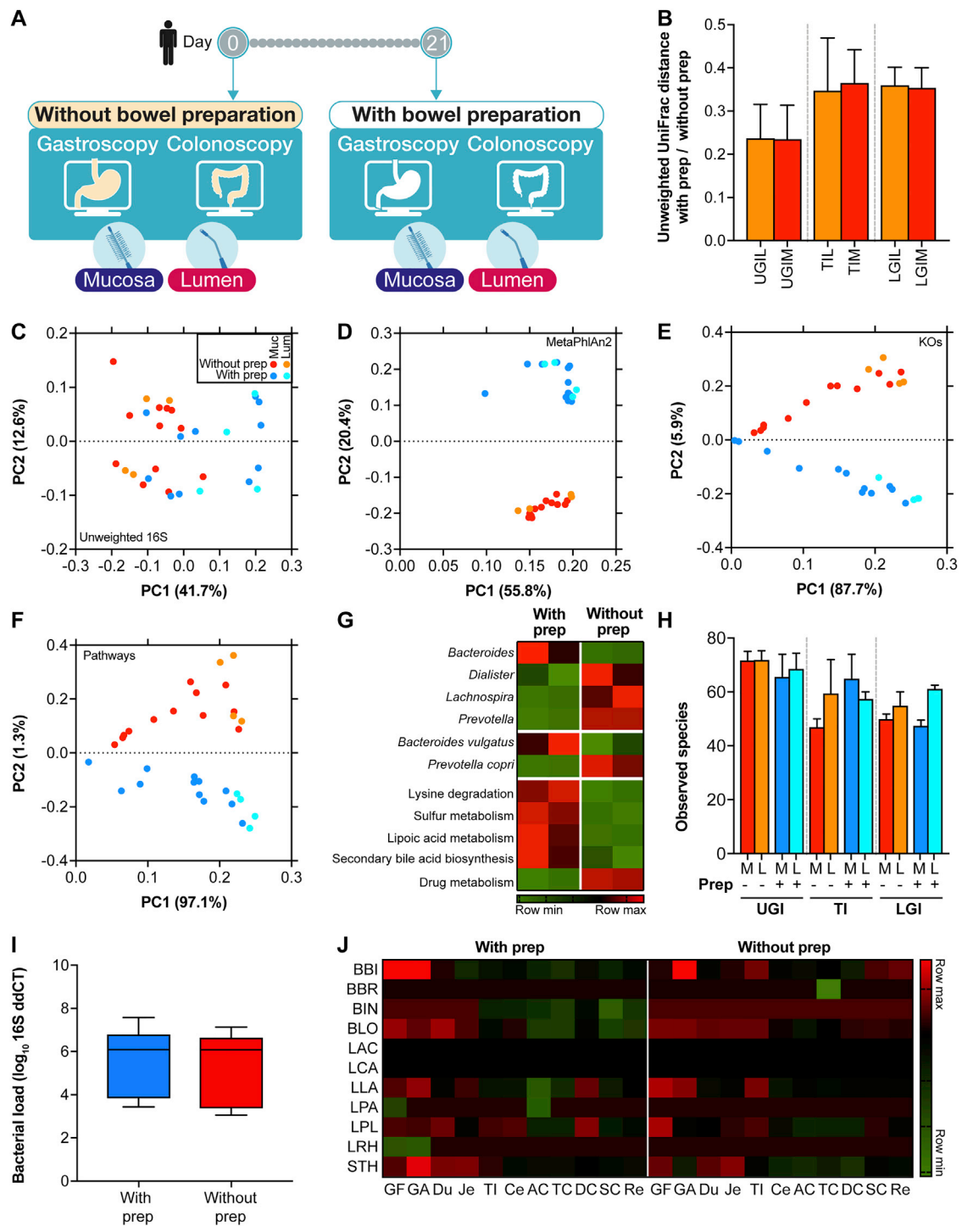
Figure S1. Murine Stool Microbiome Configuration Only Partially Correlates with the Gut Mucosa Microbiome, Related to Figure 1

(A) Scheme of the gastrointestinal regions sampled from 14 weeks old male C57BL/6 mice housed at the Weizmann institute SPF animal facility for 6 weeks without intervention (n = 10). (B-C) Unweighted UniFrac distances between upper gastrointestinal (UGI), lower gastrointestinal (LGI) and stool samples in a (B) PCoA and (C) quantification of distances to stool. Significance: One-way ANOVA & Tukey post hoc. (D) Global taxonomic differences. (E-G) Significant differences in composition between (E) UGI and LGI (F) LGI mucosa and stool (G) LGI lumen and stool in red (q < 0.1). Significance: FDR-corrected Mann-Whitney. (H-I) Taxa significantly different between lumen and mucosa in the (H) UGI and (I) LGI. Significance: Mann-Whitney. (J) Per anatomical region abundance of taxa significantly different from stool. Significance: Two-Way ANOVA & Dunnett. (K) alpha diversity. Significance: Mann-Whitney. (L) qPCR of bacterial load normalized to a detection threshold of 40. Significance: Mann-Whitney. ST, stomach; DU, duodenum; PJ, proximal jejunum; DJ, distal jejunum; IL, ileum; CE, cecum; PC,

(legend continued on next page)

proximal colon; DC, distal colon. UGI, upper gastrointestinal tract; LGI, lower gastrointestinal tract. Muc, mucosa; Lum, Lumen. Symbols represent the mean, error bars SEM. *$p < 0.05$; **$p < 0.01$; ***$p < 0.001$; ****$p < 0.0001$.
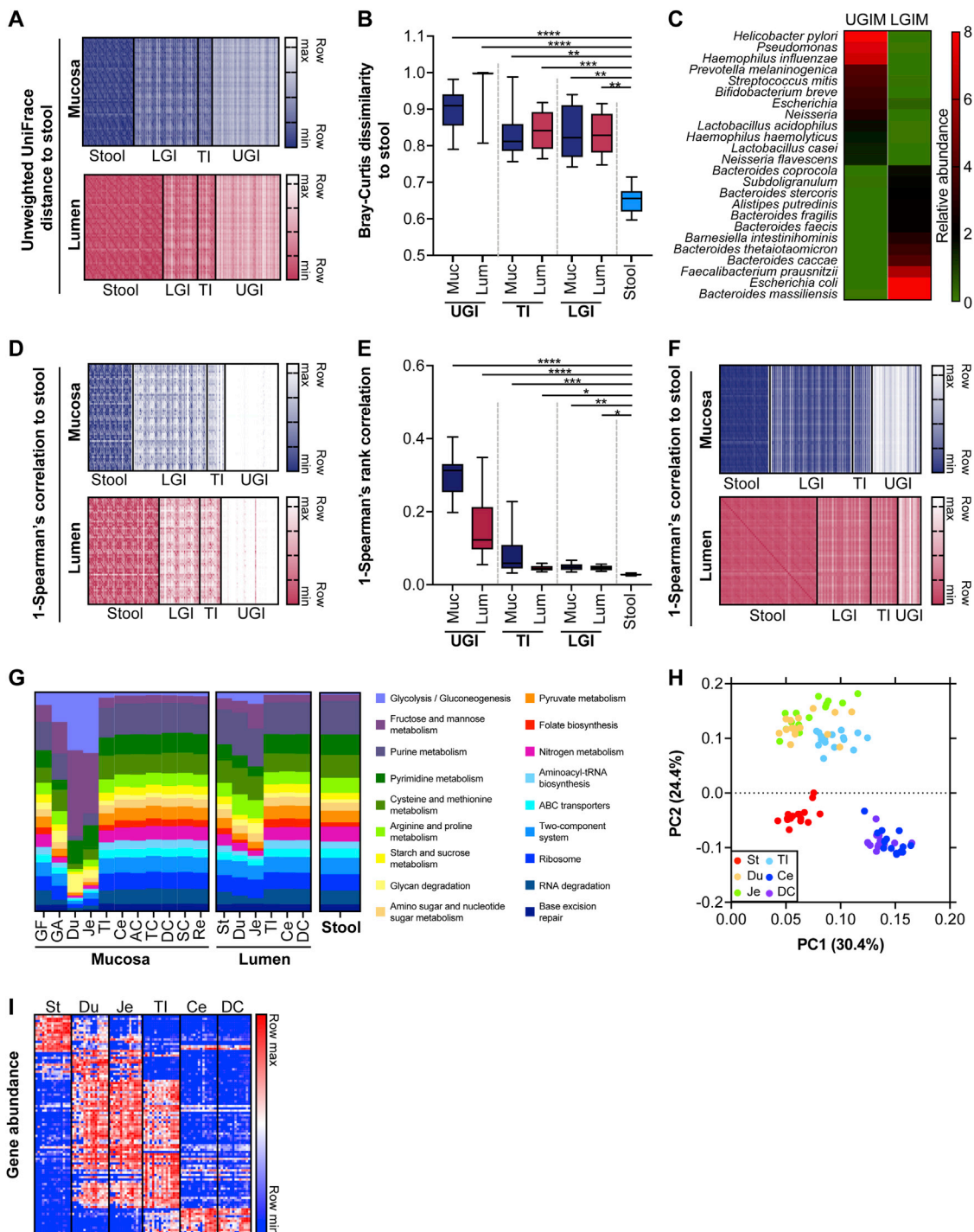
Figure S2. Bowel Preparation Alters the Human Gut Microbiome Composition and Function, Related to Figure 1

(A) Experimental outline in humans. Two healthy female participants (aged 25 and 27, BMI 20.3 and 22.8, respectively) underwent two consecutive colonoscopies. The first was performed in the absence of any form of bowel preparation, followed by a second procedure 3 weeks later performed using a routine Picolax bowel preparation protocol. (B) 16S rDNA sequencing-based unweighted UniFrac distances between the gut microbiome in prepped and non-prepped samples, paired by anatomical region (n = 2). (C) Principal coordinate analysis (PCoA) separating prepped and non-prepped LGI endoscopic samples. (D-F) Same as (C) for (D) MetaPhlAn2-, (E) KEGG orthologous (KO) genes and (E) functional pathways-based PCAs. (G) Features that differed in prepped and non-prepped LGI mucosa, based on 16S and shotgun metagenomic sequencing. (H) 16S-based alpha diversity and (I) bacterial load as determined by qPCR of the 16S rDNA global primer in the UGI, TI and LGI. (J) Species-specific qPCR of probiotics in mucosal samples throughout the human GI tract. BBI, *Bifidobacterium bifidum*;

(legend continued on next page)

BBR, *Bifidobacterium breve*; BIN, *Bifidobacterium infantis*; BLO, *Bifidobacterium longum*; LAC, *Lactobacillus acidophilus*; LCA, *Lactobacillus casei*; LLA, *Lactococcus lactis*; LPA, *Lactobacillus paracasei*; LPL, *Lactobacillus plantarum*; LRH, *Lactobacillus rhamnosus*; STH, *Streptococcus thermophilus*. GF, gastric fundus; GA, gastric antrum; Du, duodenum; Je, jejunum; TI, terminal ileum; Ce, cecum; AC, ascending colon; TC, transverse colon; DC, descending colon; SC, sigmoid colon; Re, rectum. UGI, upper gastrointestinal tract; LGI, lower gastrointestinal tract.

Figure S3. Human Fecal Microbiome Is a Limited Indicator of Gut Mucosa-Associated Microbiome Composition and Function, Related to Figure 1

(A) 16S rDNA sequencing-based unweighted UniFrac distance matrix between stool and the gut microbiome in the UGI, TI and LGI lumen and mucosa. (B) Shotgun sequencing-based Bray-Curtis dissimilarity between stool and GI lumen and mucosa samples (MetaPhlAn2). Quantification of distances to stool according to Kruskal-Wallis & Dunn's. (C) Top 24 species with the greatest (absolute) fold differences in abundance between UGI mucosa and LGI mucosa by MetaPhlAn2, paired by participant. (D-G) Shotgun metagenomic sequencing-based analysis of bacterial KEGG orthologous (KO) genes and functional pathways for fecal and gut microbiome. (D) Spearman's rank correlation matrix between stool and GI lumen and mucosa samples. (E) Quantification of 1-Spearman's rank correlations between KEGG pathway abundance in endoscopic samples to stool according to Kruskal-Wallis & Dunn's, and (F) distance matrix. (G) Relative

(legend continued on next page)

abundances of the ten most common KEGG pathways in each anatomical region and stool. (H) Principal component analysis (PCA) plot depicting clustering of the human transcriptome by various anatomical regions along the gastrointestinal tract. (I) Heatmap of the 100 most variable genes between anatomical regions. UGI, upper gastrointestinal tract; TI, terminal ileum; LGI, lower gastrointestinal tract. Muc, mucosa; Lum, Lumen. St, stomach; Du, duodenum; Je, jejunum; Ce, cecum; DC, descending colon. Symbols represent the mean, error bars SEM. *p < 0.05, **p < 0.01; ***p < 0.001; ****p < 0.0001.
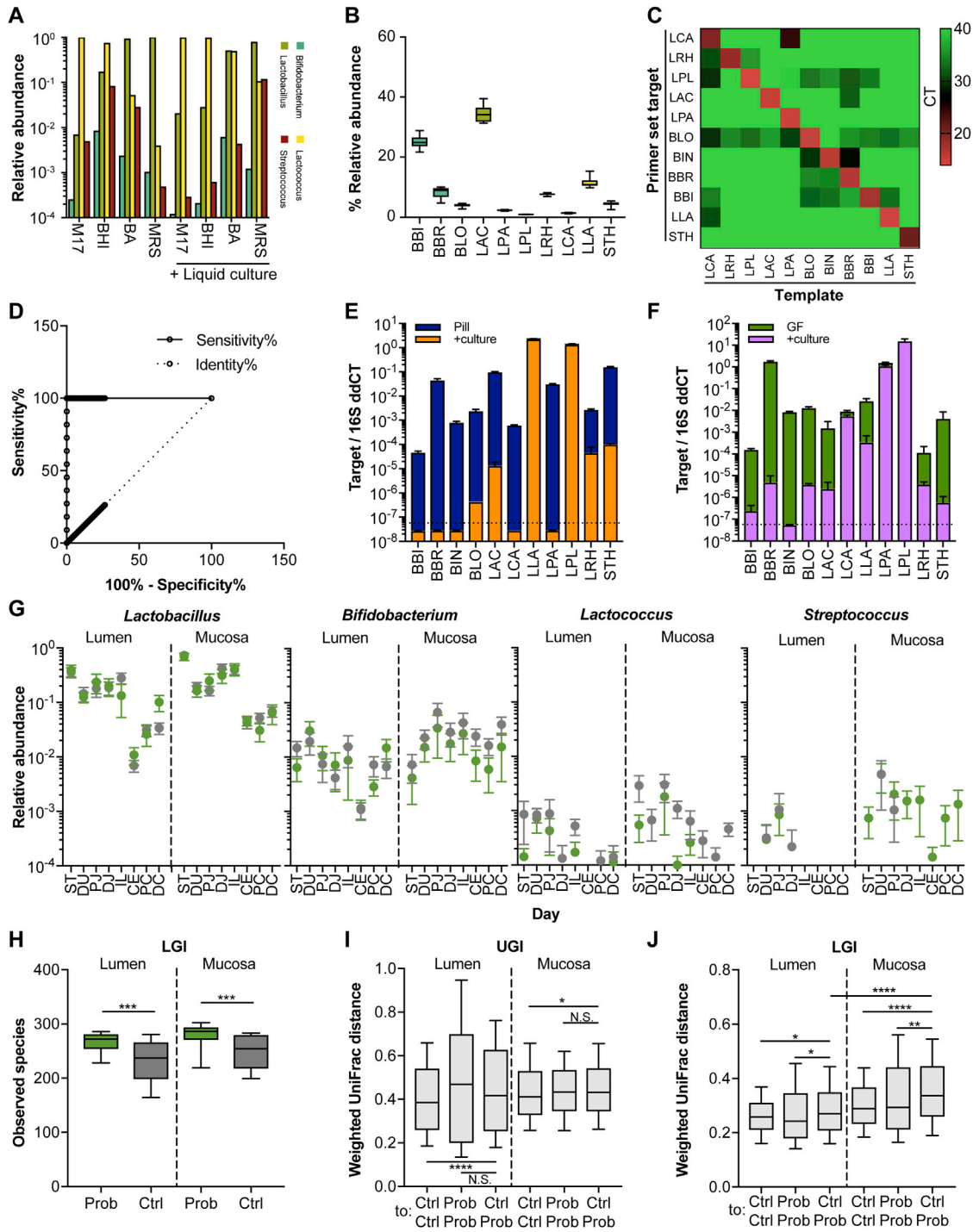
Figure S4. Probiotic Strain Assessment, Related to Figures 2 and 3 and Star Methods

(A) Quantification of live bacteria genera cultured from a probiotic pill on selective and non-selective media by 16S rDNA sequencing. (B) Probiotic pill composition by shotgun sequencing. (C) qPCR amplification of probiotics strains target in templates obtained from pure cultures. (D) Receiver-operator curve of the CT values obtained from true and mismatched pairs of C. (E and F) qPCR-based enumeration of bacteria derived from probiotics pill (E) and stool samples of ex-GF mice (F) either with or without culturing. (G) SPF mice were gavaged daily with probiotics (green) or remained untreated (gray) for 28 days. Relative abundance of probiotics genera was determined by 16S rDNA sequencing in GI tract tissues during the last day. (H-J) The following metrics were recalculated after omitting the 4 probiotics genera (*Lactobacillus, Bifidobacterium, Lactococcus, Streptococcus*) from the analysis, renormalizing relative abundances to one and re-rarefying to

(legend continued on next page)

5000. (H) Alpha diversity in the LGI. Significance: Mann-Whitney. (I and J) Weighted UniFrac distances in tissues of the (I) UGI or (J) LGI. Significance for (I and J) according to Kruskal-Wallis & Dunn's. ST, stomach; DU, duodenum; PJ, proximal jejunum; DJ, distal jejunum; IL, ileum; CE, cecum; PC, proximal colon; DC, distal colon. Symbols and horizontal lines represent the mean, error bars SEM or 10-90 percentiles. *p < 0.05; **p < 0.01; ***p < 0.001; ****p < 0.0001. N.S., non-significant. The mouse experiment was repeated 3 times.
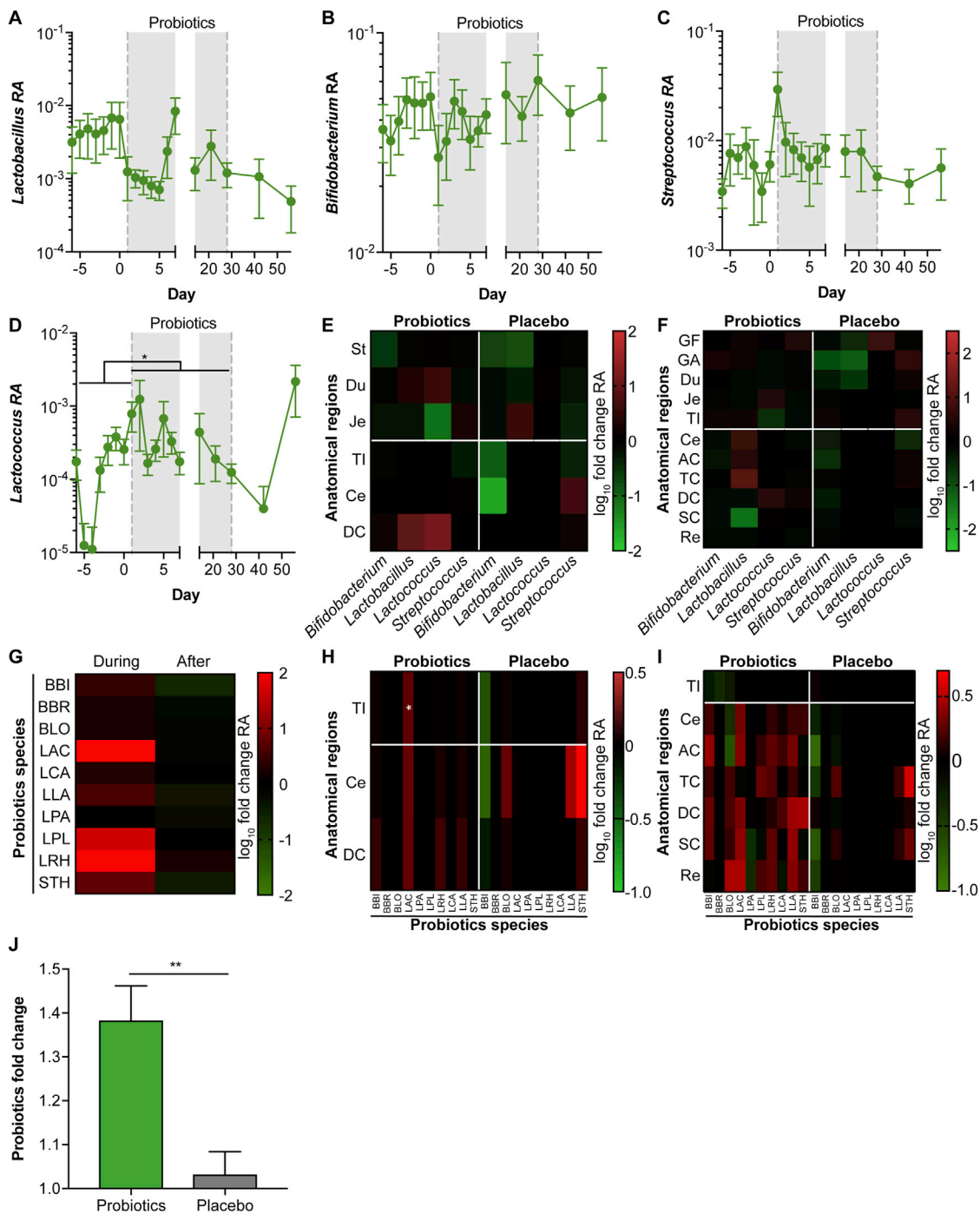
Figure S5. Quantification of Probiotics in Human Samples, Related to Figure 4

(A-D) 16S rDNA sequencing-based detection of probiotic genera in stool before, during and after supplementation: (A) *Lactobacillus*, (B) *Bifidobacterium*, (C) *Streptococcus* and (D) *Lactococcus*. Significance: Kruskal-Wallis & Dunn's for (A–D). (E and F) 16S rDNA sequencing-based detection of probiotic genera in the gastrointestinal (E) lumen and (F) mucosa for the probiotics and placebo arms. (G–I) MetaPhlAn2-based quantification of probiotic species (G) in stool, (H) in LGI lumen and (I) mucosa normalized to baseline abundances for the probiotics and placebo arms. Significance: Two-Way ANOVA & Dunnett for (E–I). (J) Aggregated probiotics load in the LGI mucosa normalized to baseline in both groups. Significance: Mann-Whitney. St, stomach; GF, gastric fundus; GA, gastric antrum; Du, duodenum; Je, jejunum; TI, terminal ileum; Ce, cecum; AC, ascending colon; TC, transverse colon; DC, descending colon; SC, sigmoid colon; Re, rectum. BBI, *Bifidobacterium bifidum*; BBR, *Bifidobacterium breve*; BIN, *Bifidobacterium infantis*; BLO, *Bifidobacterium longum*; LAC, *Lactobacillus acidophilus*; LCA, *Lactobacillus casei*; LLA, *Lactococcus lactis*; LPA, *Lactobacillus paracasei*; LPL, *Lactobacillus plantarum*; LRH, *Lactobacillus rhamnosus*; STH, *Streptococcus thermophilus*. Asterisks within a cell denote significant enrichment of a strain compared to baseline. *p < 0.05; **p < 0.01.
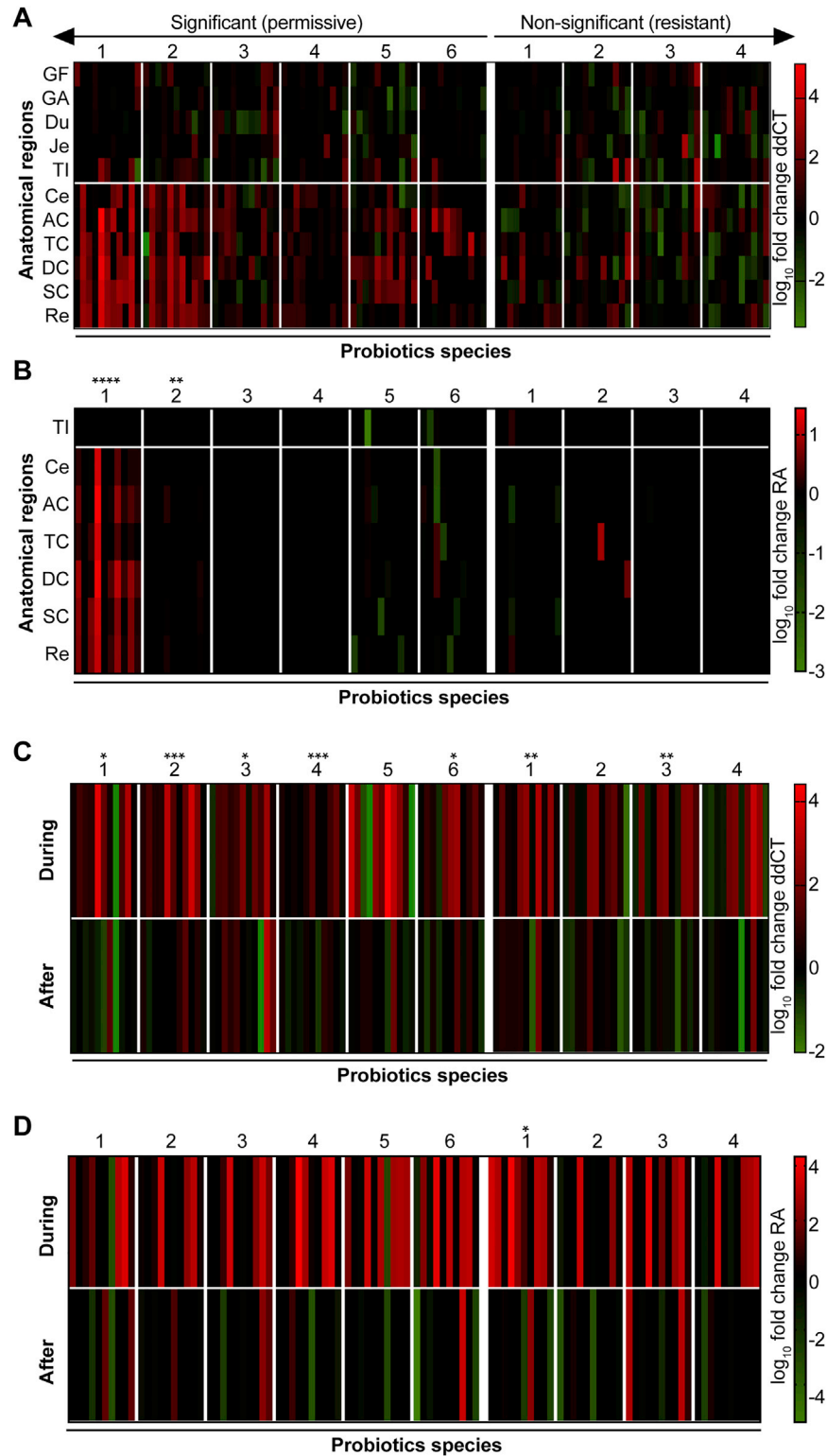
Figure S6. Human Probiotics Colonization Patterns in the GI Tract Are Not Reflected in Stool, Related to Figure 4

(A and B) Quantification of probiotics species in LGI mucosa by (A) qPCR and (B) MetaPhlAn2 3 weeks through supplementation, normalized to baseline. Significance: Mann-Whitney test for A-B. (C) qPCR quantification of probiotics species fecal shedding in supplemented individuals on day 19 of consumption and

(legend continued on next page)

1 month after probiotics cessation, normalized to baseline. (D) Same as C, but with MetaPhlAn2 on days 4-28 of consumption and 2-4 weeks following probiotics cessation. Significance: Two-way ANOVA & Dunnett for (C and D). GF, gastric fundus; GA, gastric antrum; Du, duodenum; Je, jejunum; TI, terminal ileum; Ce, cecum; AC, ascending colon; TC, transverse colon; DC, descending colon; SC, sigmoid colon; Re, rectum. Asterisks above a participant number denote a significant enrichment in overall probiotic strain abundance compared to baseline. *p < 0.05; **p < 0.01; ***p < 0.001; ****p < 0.0001.
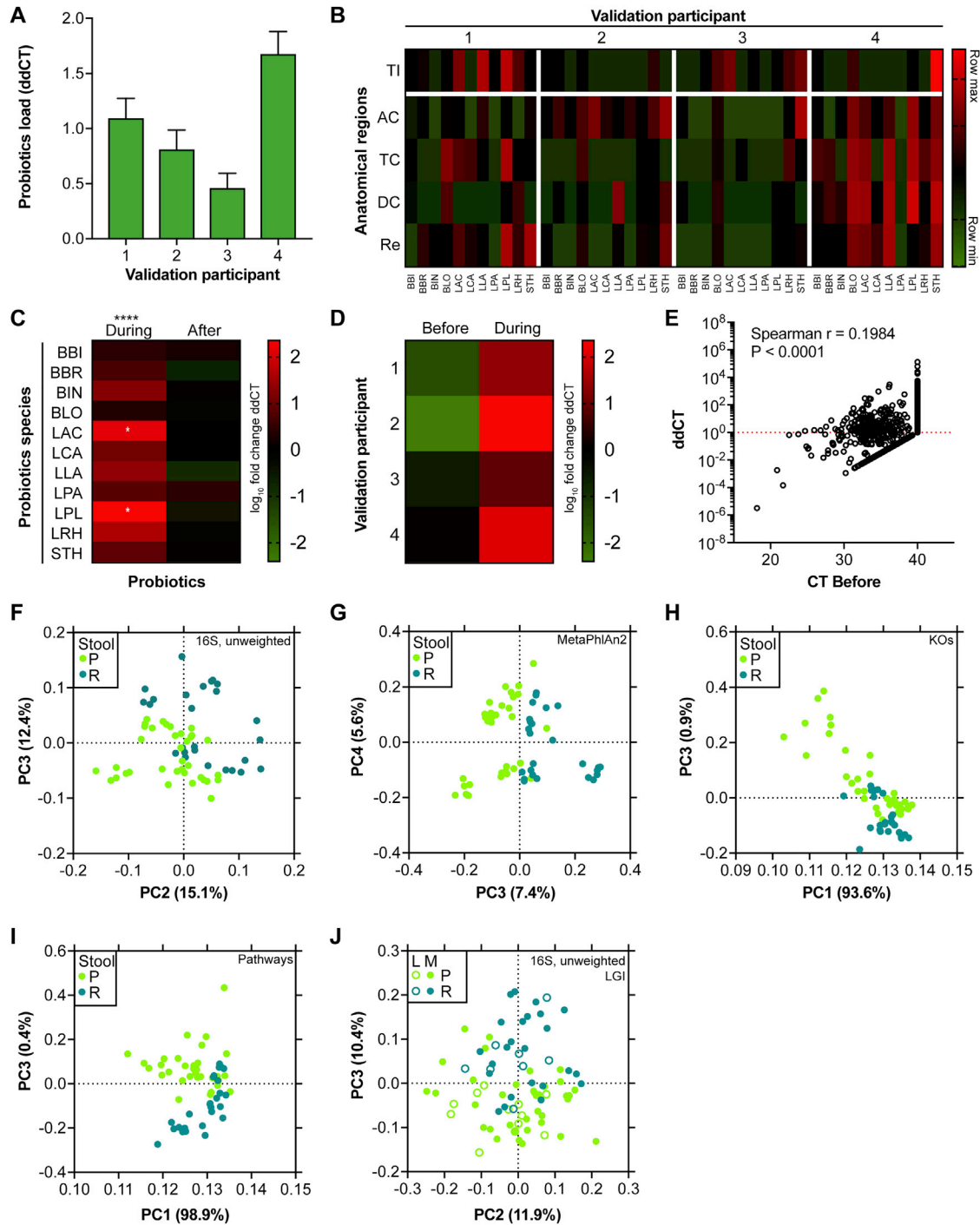
Figure S7. Validation of the Probiotics Personalized Effects in a Second Human Cohort, Related to Figures 4 and 5

(A–D) Four individuals consumed probiotics according to the same protocol described in Figure 4, and underwent a colonoscopy after 21 days of probiotics supplementation. Probiotics load is quantified using qPCR. (A) Aggregated probiotics load in the GI mucosa (TI and LGI) per participant, normalized to a detection threshold of 40. (B) Same as (A), but per species per region. (C) Shedding of probiotics in stool on day 19, and 1 month post probiotics-cessation (day 56). *p < 0.05; ****p < 0.0001, Two-Way ANOVA & Dunnett. (D) Aggregated probiotics load in stool per participant. (E) Spearman's correlation between the initial bacterial load of a probiotic target in a specific mucosal niche and its fold change after probiotics supplementation, as determined by qPCR. (F-G) 16S-based PCoA of (F) unweighted UniFrac distances separating stool microbiome composition of probiotics-permissive (P) from resistant (R) individuals prior to probiotics supplementation (p < 0.0001). (G) Same as (F) for MetaPhlAn2 PCA (p < 0.0001). (H) PCA based on bacterial KOs separating stool of probiotics-permissive

(legend continued on next page)

(P) from resistant individuals prior to probiotics consumption (p = 0.0043). (I) Same as (H) for KEGG pathways (p < 0.0001). (J) 16S-based PCoA of unweighted UniFrac distances separating LGI mucosa and lumen composition of probiotics-permissive from resistant individuals prior to probiotics supplementation (p = 0.0002). Significance: Mann-Whitney on the difference between inter- and intra-group distances for (F–J). P, permissive; R, resistant. Horizontal lines represent the mean, error bars SEM.
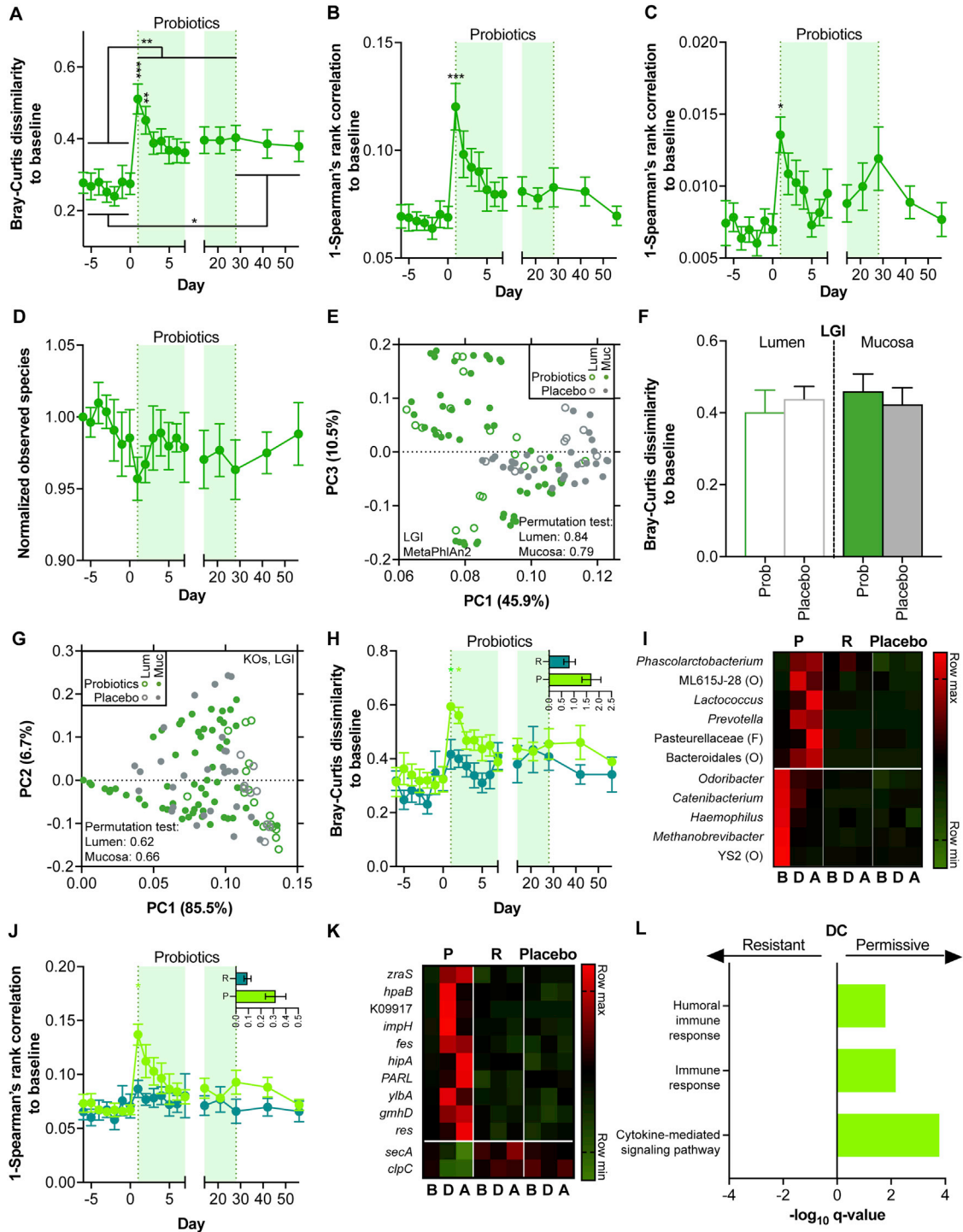
Figure S8. Global and Individual Probiotics Impacts on the Human Stool and Gut Mucosa, Related to Figures 6 and 7

(A) Shotgun sequencing-based Bray-Curtis dissimilarity indices between stool samples collected throughout the study and their respective baseline samples (MetaPhlAn2). Asterisks on horizontal lines compare periods according to a paired Friedman's test & Dunn's, excluding days 1-3. Asterisks on symbols according to Two-Way ANOVA & Dunnett to baseline. (B-C) Same as (A), but with 1-Spearman's correlation to baseline for (B) bacterial KOs and (C) KEGG pathways. (D) Same as (A), but with alpha diversity, normalized to baseline stool samples. (E) PCA based on MetaPhlAn2 in the LGI mucosa of probiotics and placebo on day 21. Significance: a permutation test. (F) Shotgun sequencing-based Bray-Curtis dissimilarity to baseline in probiotics and placebo LGI mucosa (MetaPhlAn2). (G) Same as (E), but for bacterial KOs. (H) Shotgun sequencing-based Bray-Curtis dissimilarity indices of stool samples of permissive (P) and resistant (R) individuals to their respective baseline samples. Green asterisks on symbols according to Two-Way ANOVA & Dunnett to baseline. Inset: area under the distance to baseline

(legend continued on next page)

curve during supplementation, from baseline and excluding days 1-3. Significance: Mann-Whitney. (I) Genera that changed in relative abundance in permissive individuals during (D) and after (A) probiotics consumption compared to baseline (B), but not in resistant and placebo. (J) Same as (H) with bacterial KOs and 1-Spearman's correlation (p = 0.06 for differences between areas under the distance to baseline curve). (K) Same as (I), but with KOs. (L) Host pathways that distinguish significantly between permissive and resistant individuals in the descending colon following probiotics supplementation, FDR corrected. P, permissive; R, resistant. Horizontal lines or symbols represent the mean, error bars SEM or 10-90 percentiles. *p < 0.05; **p < 0.01, ***p < 0.001.